Kidins220/ARMS binds to the B cell antigen receptor and regulates B cell development and activation

Gina J. Fiala,[1,2,3,4] Iga Janowska,[1,2,4*] Fabiola Prutek,[1,2,4*] Elias Hobeika,[1,4,11] Annyesha Satapathy,[10] Adrian Sprenger,[2,5,6] Thomas Plum,[1,2,4] Maximilian Seidl,[4,9] Jörn Dengjel,[2,5,6] Michael Reth,[1,2] Fabrizia Cesca,[10] Tilman Brummer,[2,7,8] Susana Minguet,[1,4**] and Wolfgang W.A. Schamel[1,2,4**]

[1]Department of Molecular Immunology, BioIII, Faculty of Biology, University of Freiburg and Max Planck Institute of Immunobiology and Epigenetics, 79104 Freiburg, Germany
[2]Centre for Biological Signaling Studies (BIOSS), [3]Spemann Graduate School of Biology and Medicine (SGBM), [4]Centre of Chronic Immunodeficiency (CCI), [5]Department of Dermatology, [6]Center for Biological Systems Analysis (ZBSA), [7]Institute of Molecular Medicine and Cell Research, [8]Comprehensive Cancer Centre Freiburg, and [9]Institute of Pathology, University Medical Center Freiburg, University of Freiburg, 79104 Freiburg, Germany
[10]Center of Synaptic Neuroscience, Italian Institute of Technology, 16163 Genova, Italy
[11]Institute of Immunology, University Hospital Ulm, 89081 Ulm, Germany

B cell antigen receptor (BCR) signaling is critical for B cell development and activation. Using mass spectrometry, we identified a protein kinase D–interacting substrate of 220 kD (Kidins220)/ankyrin repeat–rich membrane-spanning protein (ARMS) as a novel interaction partner of resting and stimulated BCR. Upon BCR stimulation, the interaction increases in a Src kinase–independent manner. By knocking down Kidins220 in a B cell line and generating a conditional B cell–specific Kidins220 knockout (B-KO) mouse strain, we show that Kidins220 couples the BCR to PLCγ2, Ca^{2+}, and extracellular signal-regulated kinase (Erk) signaling. Consequently, BCR-mediated B cell activation was reduced in vitro and in vivo upon Kidins220 deletion. Furthermore, B cell development was impaired at stages where pre-BCR or BCR signaling is required. Most strikingly, λ light chain–positive B cells were reduced sixfold in the B-KO mice, genetically placing Kidins220 in the PLCγ2 pathway. Thus, our data indicate that Kidins220 positively regulates pre-BCR and BCR functioning.

CORRESPONDENCE
Wolfgang W.A. Schamel:
wolfgang.schamel@
biologie.uni-freiburg.de
OR
Susana Minguet:
susana-minguet@
biologie.uni-freiburg.de

Abbreviations used: ASC, antibody-secreting cell; BAFFR, B cell–activating factor receptor; B-KO, B cell–specific KO; Btk, Bruton's tyrosine kinase; CTRL, control; DAG, diacylglycerol; Erk, extracellular signal-regulated kinase; FO, follicular; GC, germinal center; HC, heavy chain; IL-7R, IL-7 receptor; LC, light chain; mIg, membrane-bound Ig; MZ, marginal zone; MZP, MZ precursor; NP, nitrophenol; PC, peritoneal cavity; PKD, protein kinase D; WB, Western blotting.

The BCR is a multiprotein complex expressed on the surface of B lymphocytes from where it transmits critical signals for their development, proliferation, and activation. The BCR consists of two Ig heavy chains (HCs) and two light chains (LCs), forming the antigen-binding and membrane-bound Ig molecule (mIg), and the signal transduction unit composed of the *mb-1*–encoded Igα and the *B29*-encoded Igβ heterodimer (Hombach et al., 1990).

Antigen binding to mIg induces phosphorylation of cytoplasmic Igα/β tyrosines by the tyrosine kinases Lyn (Kurosaki, 1999) and Syk (Rolli et al., 2002). The subsequent recruitment of Syk to the BCR results in increased Syk activity and phosphorylation of the adaptor protein SLP65 (Wienands et al., 1998), which binds and activates the Bruton's tyrosine kinase (Btk) and the phospholipase Cγ2 (PLCγ2). PLCγ2 generates inositol 1,4,5-trisphosphate (IP_3) and diacylglycerol (DAG). IP_3 induces Ca^{2+} influx (Sugawara et al., 1997), and DAG activates the Ras guanine nucleotide exchange factor (GEF) RasGRP3 (Hashimoto et al., 1998; Oh-hora et al., 2003). RasGRP3-activated Ras stimulates the two serine/threonine kinase isoforms Raf-1 and B-Raf, leading to Mek phosphorylation and, finally, extracellular signal-regulated kinase (Erk) activation (Gold, 2000; Brummer et al., 2002). Erk induces transcription of immediate early genes, including *c-Fos* (Richards et al., 2001; Brummer et al., 2002), which together with c-Jun transcribes

*I. Janowska and F. Prutek contributed equally to this paper.
**S. Minguet and W.W.A. Schamel contributed equally to this paper.

The Rockefeller University Press $30.00
J. Exp. Med. 2015 Vol. 212 No. 10 1693–1708
www.jem.org/cgi/doi/10.1084/jem.20141271

The Journal of Experimental Medicine

numerous genes such as *CD69* (Castellanos et al., 1997; Minguet et al., 2008).

B lymphocytes arise from hematopoietic stem cells, localized in the fetal liver of the developing embryo and in the BM of young and adult mice (Rolink and Melchers, 1991). Early B cell precursors depend on IL-7 receptor (IL-7R) signaling (Cumano et al., 1990), but as soon as they express the pre-BCR (composed of the μHC, the surrogate LC, and Igα/β), pre-BCR signaling induces proliferation by activating the Ras–Erk pathway and thereby eliminates dependency on IL-7 (Fleming and Paige, 2001; Vettermann et al., 2008; Mandal et al., 2009). Indeed, mice with a defective Ras–Erk pathway exhibit a block at the early pre–B cell stage, whereas constitutively active Ras bypasses this pre-BCR checkpoint in the absence of pre-BCR expression (Shaw et al., 1999; Nagaoka et al., 2000; Yasuda et al., 2008). Rearrangement of the LC genes starts at the κ locus and only later continues at the λ locus (Arakawa et al., 1996). In mice, 90–95% of WT B cells express the κLC and only 5–10% the λLC (McGuire and Vitetta, 1981). Successful LC rearrangement leads to expression of the IgM-BCR and entry into the immature stage of development, where central tolerance is established by different mechanisms, including receptor editing (Nemazee, 2006). Then, immature B cells leave the BM and finish maturation in the spleen, where they develop from immature, transitional cells to mature follicular (FO) and marginal zone (MZ) B cells (Loder et al., 1999; Allman et al., 2001; Srivastava et al., 2005). B cell maturation, as well as survival in the periphery, requires the BCR and the B cell–activating factor receptor (BAFFR; Lam et al., 1997; Mackay et al., 1999; Gross et al., 2000; Kraus et al., 2004).

The protein kinase D (PKD)–interacting substrate of 220 kD (Kidins220), also called ankyrin repeat–rich membrane-spanning protein (ARMS), was discovered in neurons as a substrate of PKD (Iglesias et al., 2000) and, independently, as an interaction partner of the p75 neurotrophin receptor (Kong et al., 2001). Kidins220 is a large protein of 1,715 amino acids containing four transmembrane segments and cytoplasmic regions with several interaction motifs. Kidins220 binds to several receptors, such as the neurotrophin receptors TrkA, TrkB, TrkC, and p75 (Kong et al., 2001; Arévalo et al., 2004; Chang et al., 2004), a glutamate receptor (López-Menéndez et al., 2009), the VEGF receptor (Cesca et al., 2012), and the TCR (Deswal et al., 2013). The interaction of Kidins220 with TrkA increases upon stimulation and couples TrkA to Erk activation (Arévalo et al., 2004). In T cells, Kidins220 is constitutively associated with the TCR and couples the TCR to Erk activation, possibly by its interaction with Raf-1 and B-Raf (Deswal et al., 2013). Thus, Kidins220 is a scaffold protein linking several receptors to downstream signals, mainly to the Ras–Erk pathway (Neubrand et al., 2012).

Here, we identify Kidins220 as a novel interaction partner of the BCR. We analyzed this interaction biochemically and studied the relevance of Kidins220 for B cell development and activation in vitro and in vivo.

RESULTS

Kidins220 binds to the BCR in unstimulated B cells

To identify novel interaction partners of the resting BCR, we purified the IgG2a-BCR from mouse K46 B cells using protein G–coupled beads and identified bound proteins using mass spectrometry. In addition to the BCR subunits γ2aHC, κLC, and Igα, we detected Kidins220 (Fig. 1 A). Next, we tested whether Kidins220 interacts with other BCR isotypes. To this end, we made use of different transfectants of the J558L B cell line expressing nitrophenol (NP)-specific IgD-, IgM-, or IgG2a-BCRs (Hombach et al., 1988; Schamel and Reth, 2000). After lysis, BCRs were purified using NP-coupled Sepharose beads, and the copurified proteins were analyzed by SDS-PAGE and Western blotting (WB); lysates served as controls (CTRLs; Fig. 1 B). We detected association of Kidins220 with the IgD-, IgM-, and IgG2a-BCR. When J558L cells not expressing any BCR were used, Kidins220 was not detected. Kidins220 was bound to BCRs on the B cell surface (not depicted) and was associated with the BCR in primary splenic B cells from B1-8/IEKT mice expressing an NP-specific BCR (Fig. 1 C). The Igα and Igβ subunits of the BCR are dispensable for BCR's association with Kidins220 because in their absence the transmembrane form of mIgD also interacted with Kidins220 (not depicted). Furthermore, the Kidins220–BCR interaction was specific because Kidins220 was not immunopurified with MHC class I (MHCI) from B cells before (Fig. 1 D) and after anti-MHC or anti-BCR stimulation (not depicted).

Next, we asked whether BCR triggering changes the constitutive association of Kidins220 with the BCR. K46 cells expressing either NP-specific (containing the λLC) IgD- or IgM-BCRs were stimulated with anti-λLC antibodies (Fig. 1 E). NP purification of the BCRs demonstrated that the amount of Kidins220 purified with the BCR was increased upon stimulation. K46 cells not expressing an NP-specific BCR served as negative CTRL. Phosphorylation of Akt indicated that the cells were successfully stimulated.

To test whether the increased association of Kidins220 with the BCR relied on intracellular signaling, we used the Src kinase inhibitor PP2 (Hanke et al., 1996) that blocks BCR phosphorylation and downstream signaling. Indeed, phosphorylation of Erk was inhibited by PP2 pretreatment (Fig. 1 F). In contrast, PP2 did not abolish the enhanced association of Kidins220 to the IgM- or IgD-BCR upon anti-λLC stimulation. Treatment of the cells with the phosphatase inhibitor pervanadate, which induces BCR phosphorylation and downstream signaling (Campbell et al., 1995; Wienands et al., 1996), did not enhance the Kidins220–BCR interaction (Fig. 1 F). Thus, BCR-induced downstream signaling might not be involved in the increased association of the BCR with Kidins220 upon triggering. In conclusion, Kidins220 is a novel interaction partner of the IgD-, IgM-, and IgG2a-BCR isotypes (Fig. 1 G).

Kidins220 regulates signal transduction by the IgD- and the IgM-BCRs

To analyze its role in B cells, we generated IgD- and IgM-BCR–expressing K46 cell lines (K46Lδm and K46Lμm, respectively)

A

protein name	protein ID	no. of unique peptides	description
γ2a HC	P01863	4	BCR component
κLC	Q9JL80	4	BCR component
Igα	P11911	5	BCR component
Kidins220/ ARMS	E9Q9B7	2	Kinase D-interacting substrate of 220 kDa / Ankyrin repeat-rich membrane spanning protein

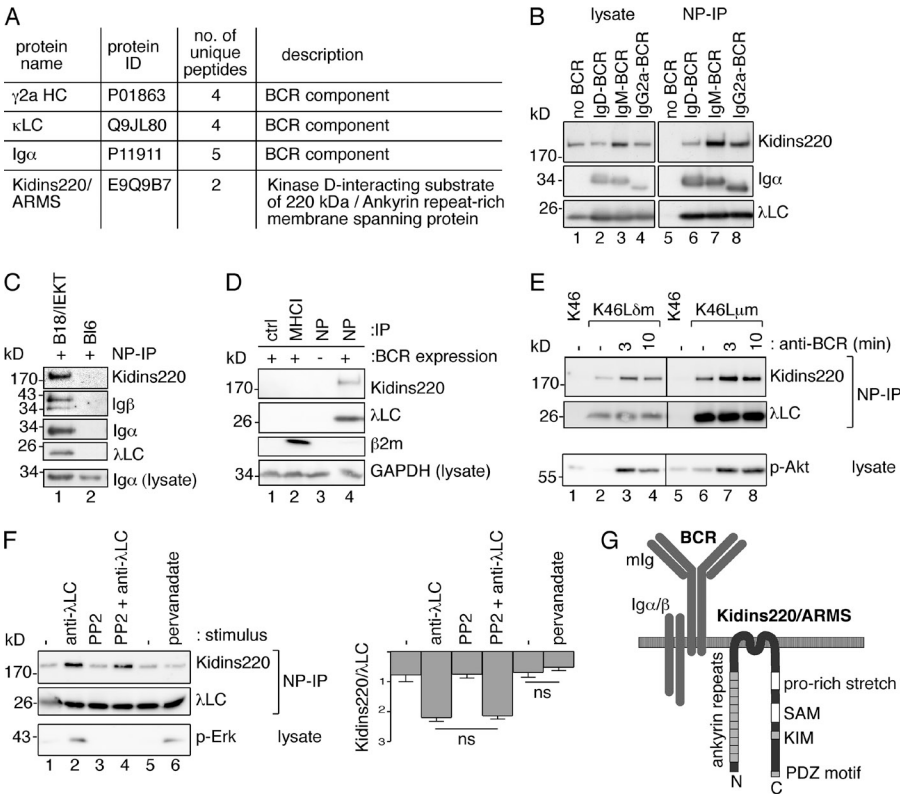

Figure 1. Kidins220 constitutively associates with different BCR isotypes. (A) IgG2a-BCR was purified from resting K46 B cells, and bound proteins were identified by tandem mass spectrometry. (B) BCRs from J558L cells expressing the indicated NP-specific BCR isotypes were purified using NP-coupled Sepharose beads, separated by reducing SDS-PAGE, and developed by WB as indicated ($n = 4$). (C) Purified splenic B cells from B1-8/IEKT mice expressing a transgenic BCR specific for NP (lane 1) and from WT C57BL/6 mice (lane 2) were lysed, and proteins were NP purified and analyzed as in B ($n = 3$). (D) Unstimulated IgD-BCR–expressing J558Lδm/mb1flN cells (lanes 1, 2, and 4) and no BCR-expressing J558L cells (lane 3) were lysed. MHCI was purified with an anti-MHCI antibody and the BCR with NP-beads, and a CTRL purification using isotype CTRL antibody–coupled beads was performed. The corresponding lysates demonstrate the same sample input for the different purifications ($n = 3$). (E) K46, K46Lδm, and K46Lμm cells were kept unstimulated (−) or were stimulated at 37°C with 3 µg/ml anti-λLC antibodies for 3 or 10 min. Proteins were NP purified and analyzed as in B. In addition, anti–phospho-Akt WB was performed using the lysates ($n = 3$). (F) K46Lμm cells were treated with 20 µM PP2 for 30 min at 37°C where indicated. Then cells were kept unstimulated (−) or stimulated for 3 min with either 3 µg/ml anti-λLC or with 25 µM pervanadate. Proteins were purified and analyzed as in B, and phospho-Erk was detected in lysates. Lanes 1 and 5 are duplicates. The quantification of the band intensities is shown (mean ± SEM, $n = 3$). Paired two-tailed Student's t test (ns, $P > 0.05$). (G) Schematic picture of the BCR–Kidins220 interaction. The ankyrin repeats, proline-rich stretch, SAM (sterile α-motif) domain, KIM (kinesin light chain–interacting motif), and PDZ (PSD-95, Discs-large, ZO-1)-binding motif are indicated.

in which Kidins220 was stably knocked down by four different Kidins220-specific shRNAs using lentiviral vectors. The shRNA #2 resulted in the strongest reduction in Kidins220 protein expression and copurification with the BCR (not depicted). Hence, the shRNA #2 (shKidins220) and a scrambled CTRL shRNA cell line (shScrambled; Fig. 2 A for K46Lδm and Fig. 3 A for K46Lμm) were used for all further experiments.

Because BCR expression was not impaired in the shKidins220 cells (not depicted), we stimulated the cells and studied BCR-induced signaling events. When the BCR was triggered, up-regulation of CD69, an early B cell activation marker, by K46Lδm cells was nearly absent upon Kidins220 knockdown (Fig. 2 B). Furthermore, the shKidins220 cells showed less Ca^{2+} influx upon BCR stimulation than the CTRL cells (Fig. 2 C for K46Lδm and Fig. 3 D for K46Lμm). Thus, Kidins220 is required for optimal BCR-induced activation of K46 B cells expressing an IgD- or IgM-BCR.

CD69 up-regulation in B cells is controlled by the Ras–Erk pathway (Minguet et al., 2005). To test whether Kidins220 is involved in coupling the BCR to Raf-1 and B-Raf, the IgD-BCR on shScrambled and shKidins220 cells was stimulated with the anti-idiotypic antibody Ac146. Raf-1 and B-Raf were immunopurified and analyzed by WB (Fig. 2 D). BCR stimulation led to Raf-1 dephosphorylation at the inhibitory residue serine259 (S259; Rodriguez-Viciana et al., 2006) and an increase in phosphorylation at S338, which is critical for Raf-1 activation (Mason et al., 1999; Brummer et al., 2002; Dhillon et al., 2002). In contrast to shScrambled cells, Raf-1 did not display these dynamic changes in phosphorylation in shKidins220 cells. Furthermore, in shScrambled, but not in shKidins220 cells, we detected a decreased electrophoretic mobility of Raf-1 and B-Raf upon BCR stimulation, which reflects several feed-forward and feedback phosphorylation events occurring on both isoforms (Brummer et al., 2003; Dougherty et al., 2005). Together, these data indicate that functional coupling of the BCR to both Raf kinases is enhanced by Kidins220.

Upon stimulation, Raf proteins activate Mek and Mek phosphorylates Erk. Indeed, BCR-induced Mek and Erk phosphorylations were reduced in shKidins220 cells (Fig. 2 [E and F] for K46Lδm and Fig. 3 [B and C] for K46Lμm). A similar result was obtained when the cells were stimulated with antigen nitroiodophenol (NIP)–coupled BSA (not depicted), further supporting that Kidins220 positively regulates the Erk pathway in K46 cells. Consequently, induced expression of the Erk target gene product c-Fos was strongly reduced in the shKidins220 cells (not depicted). When early signaling events upon BCR triggering were studied, phosphorylation of the two kinases

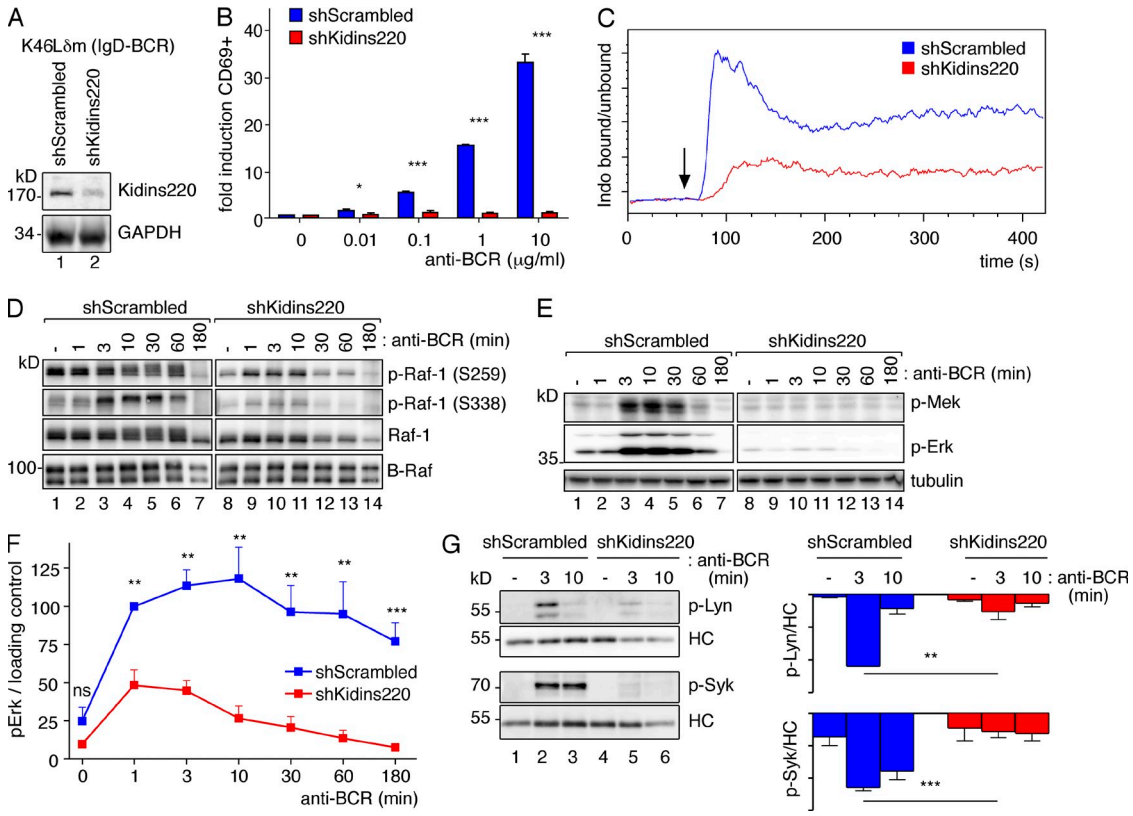

Figure 2. Kidins220 promotes signaling via the IgD-BCR in the K46 B cell line. (A) The lysates of scrambled shRNA (shScrambled) or Kidins220-specific shRNA #2 K46Lδm cells (shKidins220) were analyzed by WB as indicated ($n > 3$). (B) Cells as in A were stimulated in triplicates with increasing amounts of the anti-idiotypic antibody Ac146 for 6 h. Cells were analyzed by flow cytometry for CD69 expression. Fold induction of the percentage of $CD69^+$ cells is given ($n = 3$). The mean ± SEM is shown. Two-tailed Student's *t* test (*, $P < 0.05$; ***, $P < 0.001$). (C) Cells as in A were stained with the dye Indo-1. The ratio of Ca^{2+}-bound Indo-1 to Ca^{2+}-unbound Indo-1 was measured by flow cytometry. Stimulation was induced after 60 s of the measurement with Ac146 (arrow; $n = 3$). (D) Cells as in A were stimulated with Ac146 for the indicated time points or left untreated. After cell lysis, anti–Raf-1 (top three rows) and anti–B-Raf (bottom row) immunoprecipitations were performed and analyzed as indicated ($n = 2$). (E) Cells were treated as in D, and the lysates were analyzed by WB as indicated. (F) A quantification of the phospho-Erk/loading CTRL ratio after normalization is shown for seven independently performed experiments as in E. The mean ± SEM is plotted. Paired one-tailed Student's *t* test (ns, $P > 0.05$; **, $P < 0.01$; ***, $P < 0.001$). (G) Cells as in A were stimulated as indicated, and phosphorylated proteins were purified and analyzed by WB using the phospho-specific antibodies as indicated. A quantification is shown (mean ± SEM, $n = 3$). Paired two-tailed Student's *t* test (**, $P < 0.01$; ***, $P < 0.001$).

regulating BCR phosphorylation, Lyn and Syk, was significantly reduced in the absence of Kidins220 (Fig. 2 G for K46Lδm and Fig. 3 E for K46Lμm). However, BCR down-modulation from the cell surface upon BCR triggering was unaltered in shKidins220 cells (not depicted), demonstrating that the reduced Kidins220 levels did not globally impair B cell functioning.

Kidins220 is required for optimal B cell development in the BM

As constitutive Kidins220 deficiency (KO or $Kidins220^{-/-}$) causes embryonic lethality in mice (Cesca et al., 2012), we tested the ability of Kidins220-deficient hematopoietic precursors to develop into the B cell lineage by fetal liver adoptive transfer. Fetal liver cells were isolated from embryonic day (E) 12–14 embryos generated by mating $Kidins220^{+/-}$ mice. Similar proportions and phenotype of hematopoietic precursors were observed in Kidins220 WT and KO fetal liver cells (see Fig. 6 A). Subsequently, similar numbers of fetal liver cells from age-matched WT and KO embryos were injected into sublethally irradiated $Rag2^{-/-}\gamma c^{-/-}$ mice (Fig. 4 A). 2 mo later, the recipient mice were analyzed for B cell reconstitution. We detected lymphocytes expressing B220 in the BM of WT and Kidins220 KO fetal liver–reconstituted animals (Fig. 4 B). However, Kidins220 KO fetal liver cells were less efficient in generating $B220^+$ cells than WT CTRLs. Closer analysis of the developmental stages of $B220^+$ cells showed a slight increase of Kidins220 KO cells in the pro/pre–B cell compartment, and recirculating mature B cells were reduced (not depicted).

The reduced efficiency in generating B cells in the Kidins220 KO fetal liver–reconstituted mice could be caused by a block before B-lineage commitment. To specifically study the role of Kidins220 in B cell development, we crossed Kidins220 floxed ($Kidins220^{fl}$) mice (Cesca et al., 2011, 2012) to mb1Cre ($mb1^{Cre}$) mice. In $mb1^{Cre}$ mice, the Cre recombinase is expressed from the *mb-1* locus from the pro–B cell stage onwards (Hobeika et al., 2006). Successful deletion of both Kidins220

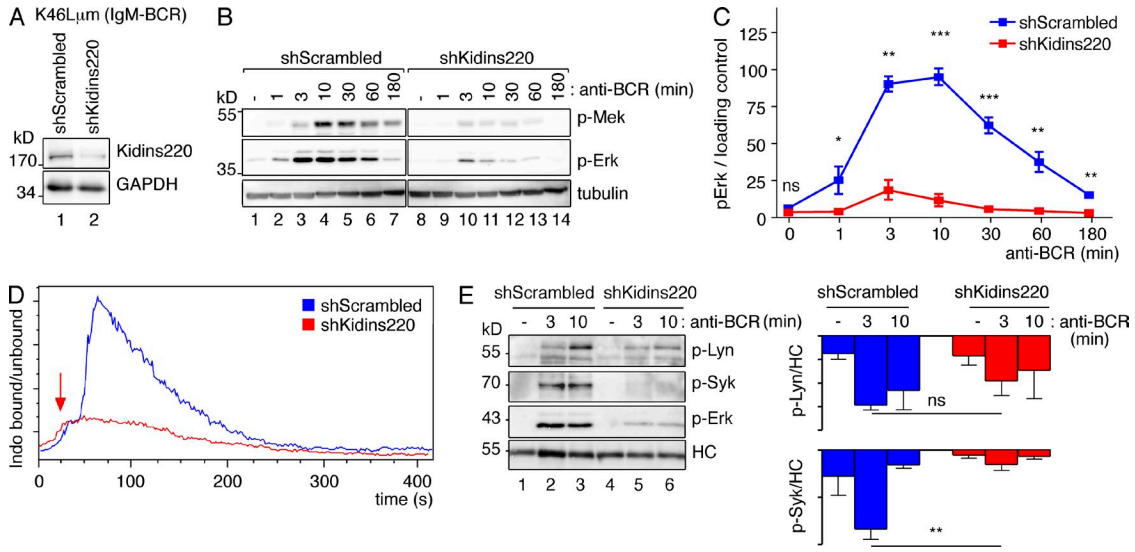

Figure 3. Kidins220 promotes signaling via the IgM-BCR in the K46 B cell line. (A) The lysates of scrambled shRNA (shScrambled) or Kidins220-specific shRNA #2 K46Lμm cells (shKidins220) were analyzed by WB as indicated ($n > 3$). (B) Cells as in A were stimulated with 10 μg/ml Ac146 for the indicated time points or left untreated. The lysates were analyzed as in Fig. 2 E ($n = 3$). (C) Quantification of the experiments shown in B (mean ± SEM). (D) Cells as in A were analyzed as in Fig. 2 C. Stimulation was induced after 50 s of the initiation of measurement with Ac146 (arrow; $n = 3$). (E) Cells as in A were treated as in Fig. 2 G, and WB was developed as indicated. A quantification is displayed (mean ± SEM, $n = 2$–3). Paired two-tailed Student's t test (ns, $P > 0.05$; *, $P < 0.05$; **, $P < 0.01$; ***, $P < 0.001$).

alleles was confirmed by PCR, and absence of the Kidins220 protein in ex vivo IL-7–expanded pro–B cells (not depicted).

The Kidins220$^{fl/-}$mb1$^{+/Cre}$ or Kidins220$^{fl/fl}$mb1$^{+/Cre}$ mice (B cell–specific KO [B-KO]) were compared with Kidins220$^{+/fl}$mb1$^{+/Cre}$ or Kidins220$^{+/-}$mb1$^{+/Cre}$ CTRLs (Fig. 4 C) because no differences were observed between mice expressing Kidins220 from one or two alleles (not depicted). Unexpectedly, ∼45% of the B-KO mice died before reaching 14 wk of life (not depicted). Those animals were smaller, weaker, and piloerected and presented with a hydrocephalus in some cases. Consequently, only healthy animals with similar body weight were used for the following analyses.

B-KO mice showed a mild but significant reduction in the relative (Fig. 4 D) and absolute (Fig. 4 E) number of B220$^+$ cells in the BM. The pro/pre–B cell compartment was percentagewise enlarged (Fig. 4 F) as the result of an increase in CD43$^+$ pro–B cells percentagewise (Fig. 4 G) and in total numbers. The total number of CD43$^-$ pre–B cells was reduced (not depicted). Furthermore, the percentage of immature cells was unchanged (Fig. 4 F). In contrast, the percentages of transitional B cells in the BM (emigrants) were significantly reduced (Fig. 4 H). Similarly, the proportion and total number of mature recirculating B cells in the BM were reduced (Fig. 3 F and not depicted).

Kidins220 KO mice possess reduced numbers of λ$^+$ B cells

Strikingly, in all B-KO cell populations in the BM, λLC expression was significantly reduced (73% reduction; Fig. 4, I and J). This deficiency became even more evident in the peripheral B cell populations (85% reduction in spleen and LNs; Fig. 5, F and I). Rearrangement of the λ locus requires a longer life span of pre–B cells (Arakawa et al., 1996) because the κ locus is activated first in the large pre–B cell stage and the λ locus rearranged only in the subsequent developmental stage (Engel et al., 1999). Hence, to test whether reduced λLC expression reflects reduced survival, we set up BM cultures supplemented with IL-7. BM cells from CTRL and B-KO mice expressed similar levels of the IL-7R CD127 and survived and proliferated to a similar extent (not depicted). In contrast, upon withdrawal of IL-7, B-KO cells showed reduced survival of IgM^{low} cells (Fig. 4 K), many of which express the pre-BCR (Rolink et al., 1991; ten Boekel et al., 1995; Ray et al., 1998), which was reflected by the relative enrichment of IgM$^+$ cells in the culture (not depicted). Because pre-BCR signals ensure survival in the absence of IL-7 (Arakawa et al., 1996), our data suggest that the reduced life span of pre–B cells, and consequently lack of λLC expression, is caused by defective pre-BCR signaling in the absence of Kindins220.

In summary, Kidins220 deficiency in the B cell lineage resulted in reduced B220$^+$ cells in the BM. The reduction of pre–B cells, together with the absence of λLC expression, might indicate reduced survival of pre–B cells that can be explained by defective pre-BCR signaling.

Kidins220 KO B cells preferentially mature to MZ B cells

Next, we analyzed the B cell compartment in peripheral lymphoid organs. The spleens of Rag2$^{-/-}$γc$^{-/-}$ mice reconstituted with Kidins220 KO fetal liver cells and of B-KO mice showed reduced CD19$^+$ cell numbers (Fig. 5 A and not depicted). To exclude the possibility that the B cells in the periphery of the B-KO mice were those without deletion, we confirmed the absence of Kidins220 WT and floxed alleles in purified splenic B cells (not depicted).

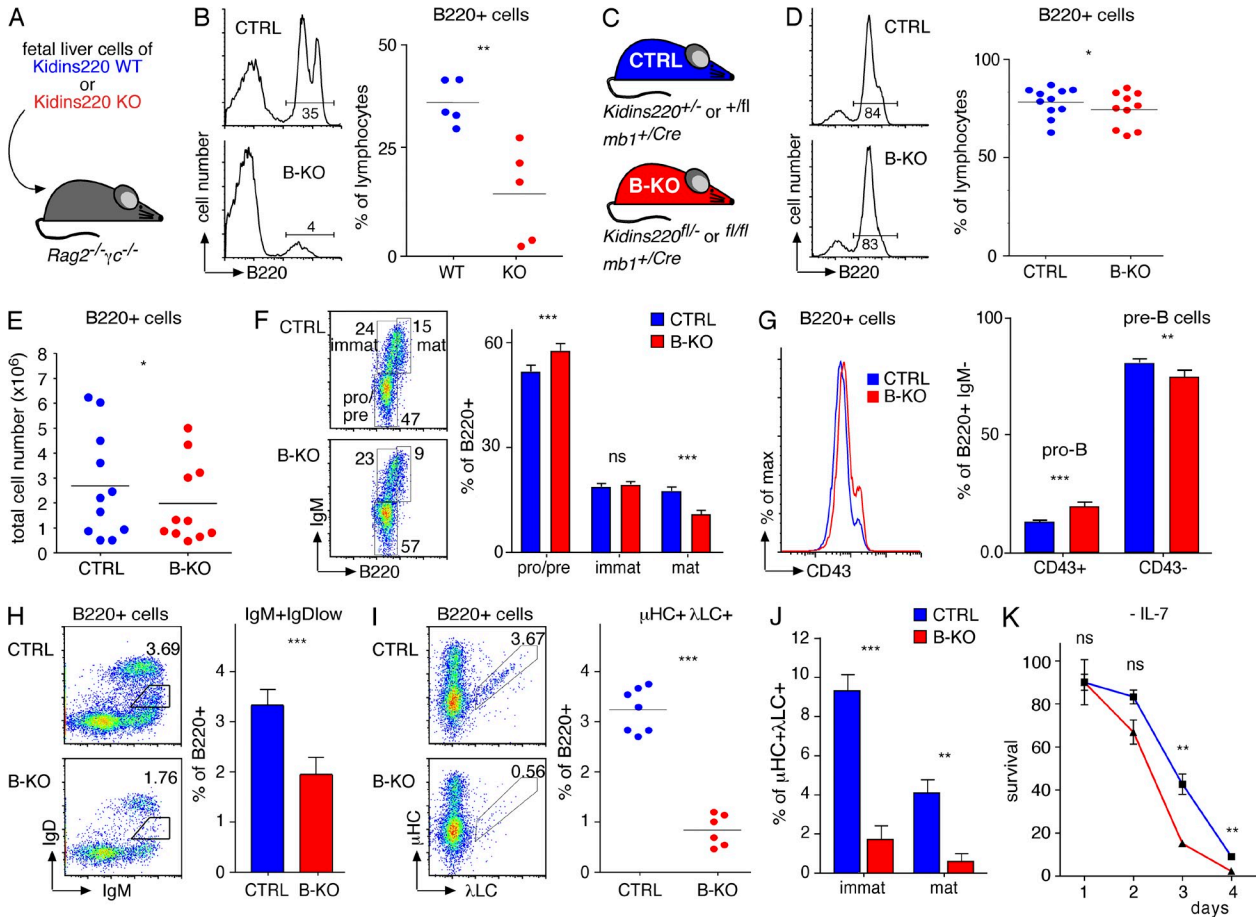

Figure 4. Early B cell development in the BM. Kidins220 is required for the development of λ+ B cells. (A) Sublethally irradiated $Rag^{-/-}\gamma c^{-/-}$ mice were reconstituted with equal numbers of WT or Kidins220 KO fetal liver cells. (B) The percentage of B220+ cells in the BM of the reconstituted mice was measured by flow cytometry (two experimental repeats, $n = 5$). (C) The genotypes of CTRL and B cell–specific Kidins220 KO (B-KO) mice are depicted. (D) An analysis of the BM of CTRL and B-KO mice using the marker B220 (left) as well as its quantification is shown (right; eight experimental repeats, $n = 10–11$). (E) The total number of B220+ cells in the BM is shown (eight experimental repeats, $n = 11$). (F) B cell development in the BM of the CTRL and B-KO mice was analyzed using anti-B220 and anti-IgM antibodies (eight experimental repeats, $n = 11$). (G) BM cells from CTRL and B-KO mice were stained using anti-B220, anti-IgM, and anti-CD43 antibodies to analyze early B cell development (eight experimental repeats, $n = 10–11$). (H) BM cells as indicated were stained using anti-B220, anti-IgM, and anti-IgD antibodies to analyze the output of B cells from the BM (seven experimental repeats, $n = 9$). (I) CTRL and B-KO B220+ BM cells were analyzed for μHC and λLC expression (four experimental repeats, $n > 6$). (J) Percentages of μHC+λLC+ cells as in I in the B220+ immature and mature gates are shown. (K) BM cells from CTRL and B-KO mice were grown for 7 d ex vivo with IL-7. Subsequently, IL-7 was removed (day 0) and the cells cultured for another 4 d. The proportion of living cells was determined by flow cytometry according to FSC/SCC and normalized to day 0 ($n > 3$). In all graphs, the mean or mean ± SEM is plotted. Paired two-tailed Student's *t* test (ns, $P > 0.05$; *, $P < 0.05$; **, $P < 0.01$; ***, $P < 0.001$).

Newly developed immature B cells pass through the transitional stages in the spleen before differentiating into mature B cells by sequential steps regulated by signals from the BCR (Rowland et al., 2010b) and through the BAFFR (Rowland et al., 2010b). The proportion of transitional B cells (gated as $CD93^+$ cells) was reduced between B-KO mice and the CTRLs (Fig. 5 B). This phenotype was recapitulated in the fetal liver adoptive transfer of Kidins220 KO cells (not depicted). B-KO mice showed increased percentages of MZ B cells and MZ precursors (MZPs) by 200% and the corresponding reduction in FO B cells (Fig. 5 C). A closer look at the MZ B cell compartment revealed that the increase in MZ B cells was accompanied by a higher proportion of MZPs (identified as $CD19^+CD93^-CD21^{high}CD23^{high}$; Srivastava et al., 2005) in B-KO mice when compared with CTRLs (Fig. 5 D). The levels of expression of the IgM- and the IgD-BCR were similar between B cells lacking or expressing Kidins220 when matched populations were compared (Fig. 5 E). λLC^+ B cells were severely reduced in the spleen (Fig. 5 F).

The fraction of B1 B cells in the spleen and in the peritoneal cavity (PC) was not altered, although the proportion of total B cells was significantly reduced; B cells in peripheral LNs were significantly decreased percentagewise and in numbers (Fig. 5, G and H; and not depicted). In addition, λLC-expressing B cells were severely reduced in the LNs (Fig. 5 I). Altogether, deletion of Kidins220 results in a reduction of

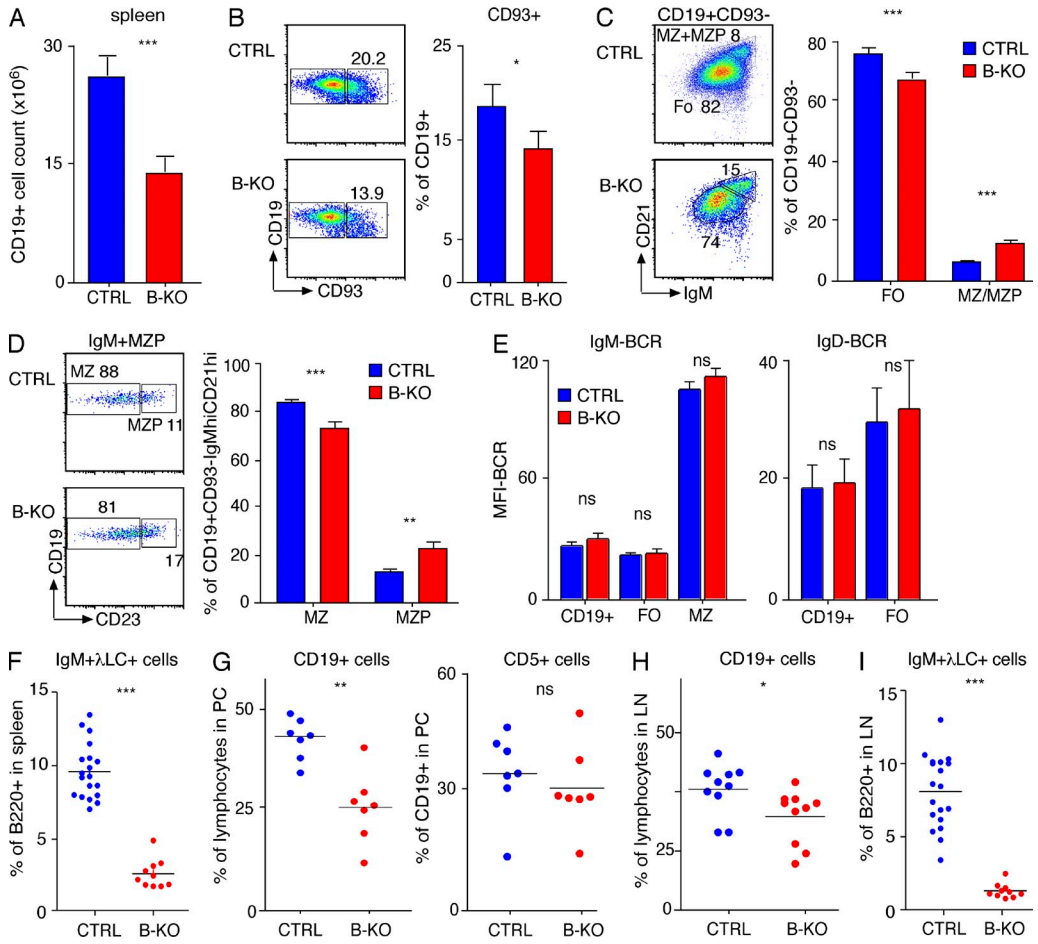

Figure 5. B cell development in the periphery. MZ B cells specifically accumulate in the absence of Kidins220. (A) Total numbers of CD19$^+$ cells in the spleen of CTRL and B-KO mice (eight experimental repeats, $n \geq 10$). (B) The percentage of CD93$^+$ transitional B cells in the spleen was quantified (six experimental repeats, $n \geq 10$). (C) MZ/MZP and FO B cell development in the spleen was analyzed by flow cytometry (six experimental repeats, $n \geq 10$). (D) Detailed analysis of the MZ B cell population (six experimental repeats, $n \geq 10$). (E) The levels of IgM- and IgD-BCR expression in matched populations were analyzed by flow cytometry ($n \geq 3$). (F) Splenic B cells were analyzed for IgM and λLC expression (six experimental repeats, $n \geq 10$). (G) The percentage of CD19$^+$ B cells (left) and their proportion of CD5$^+$ B1 cells (right) was analyzed in the PC (four experimental repeats, $n = 7$). (H) In the LNs, the percentage of CD19$^+$ B cells was analyzed (six experimental repeats, $n \geq 10$). (I) The percentage of B cells expressing the λLC was analyzed in LNs (six experimental repeats, $n \geq 10$). In all graphs, the mean or mean ± SEM is plotted. Paired two-tailed Student's *t* test (ns, $P > 0.05$; *, $P < 0.05$; **, $P < 0.01$; ***, $P < 0.001$).

B cells in peripheral lymphoid organs. In the spleen, terminal B cell maturation is altered as reflected by a skewed differentiation toward the MZ compartment.

We next investigated whether the B-KO phenotype was reproduced under competitive conditions. To this end, Rag2$^{-/-}\gamma c^{-/-}$ mice were reconstituted with Kidins220$^{-/-}$ or Kidins220$^{+/-}$ (expressing the CD45.2 marker) and WT (expressing the CD45.1 marker) fetal liver cells at a 1:1 cell ratio (Fig. 6 A). No differences in percentages or in the expression of extracellular markers (CD93, CD34, CD45, and CD19) were observed between the fetal liver cells of WT or Kidins220 KO mice (Fig. 6 A). Kidins220 KO B cells hardly developed under competition, constituting 10.9 ± 3.6% of the total B220$^+$ cells in the BM and at all maturation stages analyzed (Fig. 6, B and C). The proportion of λ$^+$ B cells was reduced; however, the limited number of Kidins220 KO B cells prevented a sound statistical analysis (Fig. 6 D). As in the BM, the percentage of Kidins220 KO B cells was clearly reduced in the periphery (15.5 ± 5.2%; Fig. 6 E). FO B cells lacking Kidins220 expression were significantly reduced and percentages of MZ B cells increased, indicating that the differentiation to MZ B cells is favored in the absence of Kidins220 (Fig. 6 F). These data strongly support a role for Kidins220 in B cell development.

B cell activation is reduced in splenic B cells from Kidins220 B-KO mice

The phenotype of the Kidins220 B-KO mice suggests a reduced capacity of the pre-BCR and BCR to generate signals important for development. To test whether BCR triggering–induced signaling was impaired in primary B cells, we performed

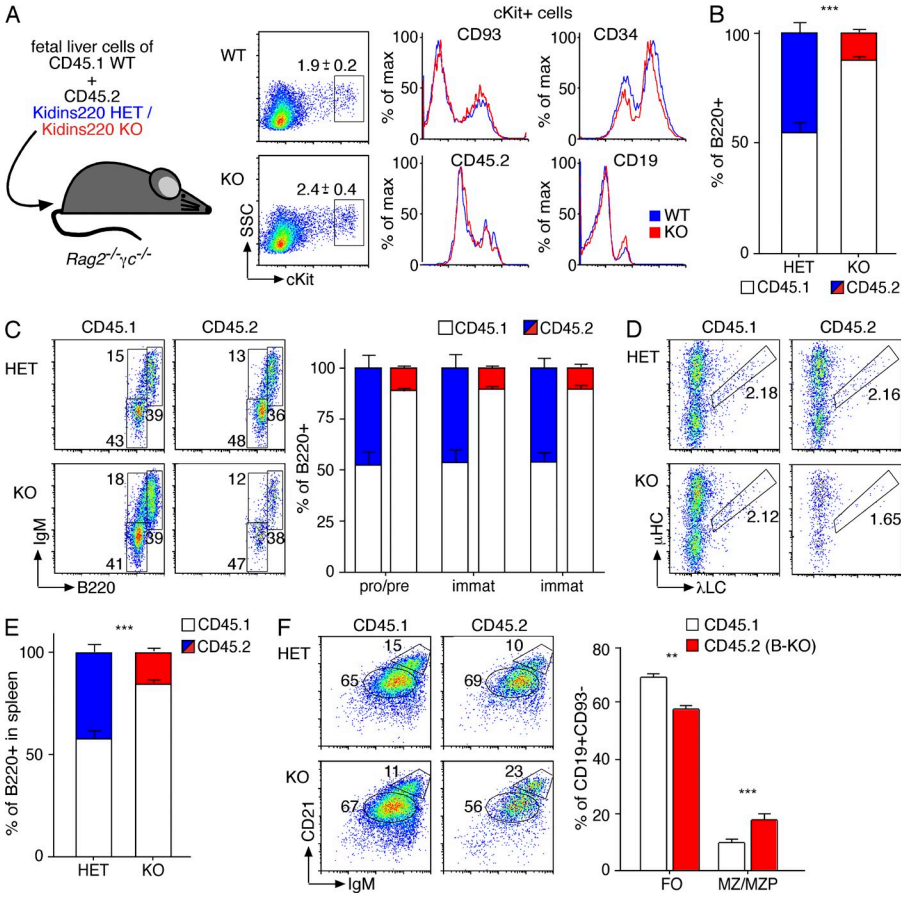

Figure 6. B cells lacking Kidins220 have a competitive disadvantage in BM repopulation. (A) Scheme of the competitive repopulation assay. Fetal liver WT cells from CD45.1 embryos were mixed with fetal liver cells obtained from Kidins220$^{+/-}$ (HET) or Kidins220$^{-/-}$ (KO) embryos from the same litter. The fetal liver cells isolated from embryos on E13.5 were analyzed by flow cytometry for percentages of hematopoietic precursors. (B) Mean chimerism in posttransplant competitive recipients transplanted with 1:1 ratios of donor (Kidins220$^{+/-}$ [blue] or Kidins220$^{-/-}$ [red], CD45.2) and competitor cells (Kidins220$^{+/+}$, CD45.1 [white]) in the BM. (C) B cell development in the BM. Representative panels and quantifications are depicted. (D) Flow cytometry analysis of μHC and λLC expression was performed; representative panels are shown. (E) Percentage of CD19^{+} cells in the spleen of the recipient mice. (F) Splenic B cell maturation was analyzed; representative dot plots and the percentages of FO and MZ/MZP B cells of mice reconstituted with 1:1 WT/Kidins220$^{-/-}$ fetal liver cells are displayed. In all graphs, the mean ± SEM is plotted (n = 6). Two-tailed Student's t test (**, P < 0.01; ***, P < 0.001).

ex vivo stimulations. First, purified splenic B cells from CTRL or B-KO mice were stimulated via the BCR using anti-IgM Fab′$_2$ antibody fragments or via TLR9 using CpG-oligodeoxynucleotides. Proliferation was measured by CFSE dilution. BCR-induced proliferation was reduced in the B-KO cells, whereas survival was not affected (Fig. 7 A and not depicted). In contrast, stimulation with CpG resulted in equal levels of strong proliferation; also proliferation in response to LPS and anti-RP105 was not diminished in B-KO cells (Fig. 7 A and not depicted), indicating that signaling from the BCR was specifically affected. BCR expression levels were similar to those of WT cells (Fig. 5 E), excluding that lower BCR levels were the cause of less BCR signaling in B-KO B cells. Second, purified B cells were stimulated with increasing concentrations of anti-IgM Fab′$_2$ and up-regulation of early activation markers was quantified by flow cytometry. B-KO cells showed a reduction in the BCR-induced expression of CD86 and CD69 (Fig. 7, B and C). Third, we measured the activation of intracellular signaling cascades upon BCR triggering in CTRL and B-KO purified splenic B cells. B-KO cells showed a reduced degree of BCR-induced Ca^{2+} influx (Fig. 7 D). Likewise, the activation of the Ras–Erk pathway, as measured by anti–phospho-Mek and anti–phospho-Erk by WB, was reduced (up to 60% reduction), and phosphorylation of Akt at its activating site S473 was slightly diminished in B-KO cells (Fig. 7 E, 30% reduction). Phosphorylation of PLCγ2 was also reduced (92% reduction) in B-KO cells, which might account for the reduced Ca^{2+} influx observed. When B cells obtained from the mixed reconstituted mice (Fig. 6 A) were stimulated ex vivo, CD86 and CD69 up-regulation was only impaired in those cells lacking Kidins220 expression (Fig. 8).

Collectively, these data suggest that Kidins220 is involved in initiating BCR signaling and, in particular, in coupling the BCR to the Ras–Erk and Ca^{2+} pathways in primary mature B cells, thereby being a positive regulator of B cell activation. In contrast, activation of the PI3K pathway and cell survival upon BCR triggering might not strongly depend on Kidins220.

B cell immune responses are impaired in Kidins220 B-KO mice

To investigate whether the reduction of λ^{+} B cells in the B-KO mice is physiologically relevant, we immunized CTRL and B-KO mice with NP-coupled KLH (NP-KLH). Importantly, primary immune responses driven by the hapten NP are accounted by BCRs carrying the λLC (Reth et al., 1978). Kidins220 deletion in B cells reduced the germinal center (GC) reaction in the B-KO mice after 6 d of immunization (Fig. 9 A). Furthermore, the B-KO mice generated less NP-specific IgG1 class-switched B cells than the CTRL mice (Fig. 9 B) and reduced anti-NP IgM and IgG serum antibody titers (Fig. 9 C). These results could be explained by a reduction in the number of NP-recognizing B cells or by defective antigen-induced B cell activation in vivo.

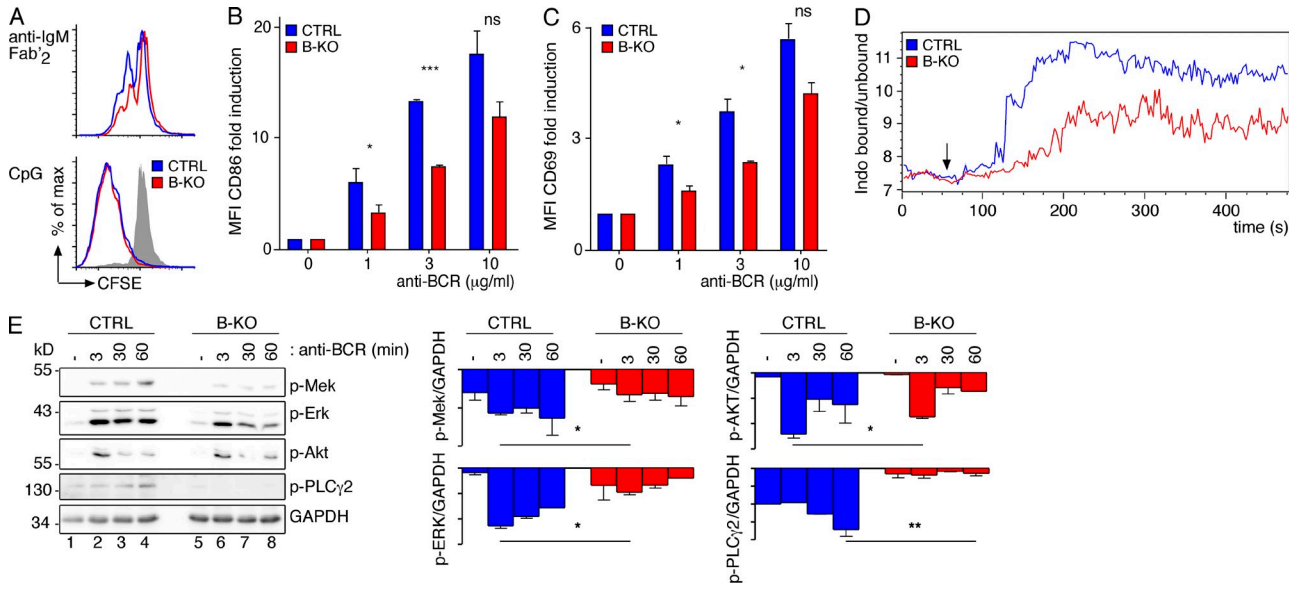

Figure 7. Kidins220 promotes signaling via the BCR in primary B cells. (A) CFSE-labeled splenic B cells from CTRL and B-KO mice were stimulated with 1 μg/ml anti-IgM Fab′$_2$ fragments or 2.5 μg/ml CpG or left untreated (gray shaded). After 3 d the proliferation-induced dilution of the CFSE dye was measured by flow cytometry (three experimental repeats, $n = 5$). (B and C) Cells as in A were stimulated with anti-IgM Fab′$_2$ fragments for 11 h and analyzed by flow cytometry using anti-CD86 (B) and anti-CD69 (C) antibodies. After normalization to the unstimulated cells, the fold induction of the mean fluorescent intensity (MFI) is shown (three experimental repeats, $n = 5$). (D) Ca^{2+} influx of the cells as in A was measured as in Fig. 2 D. Stimulation was induced with 1 μg/ml anti-IgM Fab′$_2$ fragments (arrow; two experimental repeats). (E) Cells as in A were stimulated with 3 μg/ml anti-IgM Fab′$_2$ fragments for the given time points and lysed, and proteins were separated by SDS-PAGE. Phospho-Mek, phospho-Erk, phospho-Akt, phospho-PLCγ2, and GAPDH were detected by WB (two to three experimental repeats). In all graphs, mean ± SEM is plotted. Paired two-tailed Student's *t* test (ns, $P > 0.05$; *, $P < 0.05$; **, $P < 0.01$; ***, $P < 0.001$).

To distinguish between these two possibilities and because B cell activation ex vivo was impaired in the absence of Kidins220, we were prompted to identify an antigen whose recognition was not based on the presence of the λLC. When we used the hapten TNP coupled to KLH to immunize CTRL mice, we found that 82.4% of the antibody-secreting cells (ASCs) present in the spleen secreted κ^+ antibodies correlating with the proportion of $IgM^+\kappa^+$ cells in the spleen of these mice (81.7 ± 1.3%; not depicted). Thus, we performed two immunizations using CTRL and B-KO mice: (1) TNP-coupled Ficoll, inducing T-independent type II responses, and (2) TNP-coupled KLH, inducing T-dependent responses.

The T-independent TNP-Ficoll immunization revealed reduced numbers of ASCs for IgM and IgG (Fig. 9 D) and reduced TNP-specific IgM and IgG3 serum titers in B-KO mice when compared with CTRLs at day 7 after immunization (Fig. 9 E). Likewise, the "early" TNP-KLH immune responses (namely anti-TNP IgM ASC and anti-TNP IgM serum titers) were impaired in B-KO mice when compared with CTRLs (Fig. 9, F and G, left). In contrast, in the TNP-KLH

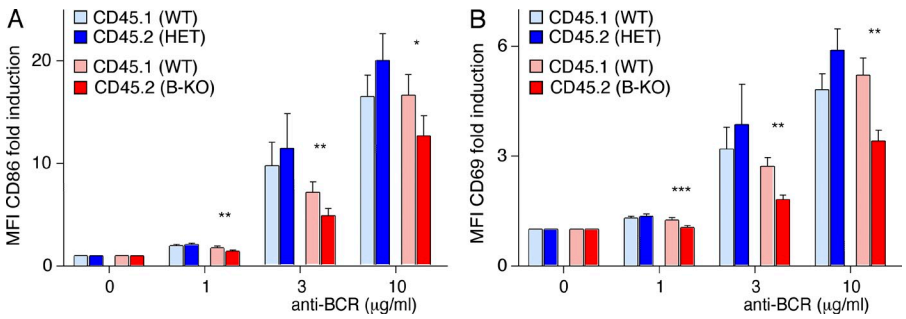

Figure 8. After competitive transfer, Kidins220 promotes primary B cell activation ex vivo. (A and B) Splenic B cells from competitive recipient mice transplanted with 1:1 ratios of fetal liver derived from either Kidins220$^{+/-}$ (HET, CD45.2, blue) and Kidins220$^{+/+}$ (WT, CD45.1, light blue) or Kidins220$^{-/-}$ (B-KO, CD45.2, red) and Kidins220$^{+/+}$ (WT, CD45.1, light red), as described in Fig. 6 A, were stimulated with anti-IgM Fab′$_2$ fragments for 11 h and analyzed by flow cytometry using anti-CD86 (A) and anti-CD69 (B) antibodies. After normalization to the unstimulated cells, the fold induction of the mean fluorescent intensity (MFI) as mean ± SEM is shown. Paired two-tailed Student's *t* test (*, $P < 0.05$; **, $P < 0.01$; ***, $P < 0.001$; $n = 6$).

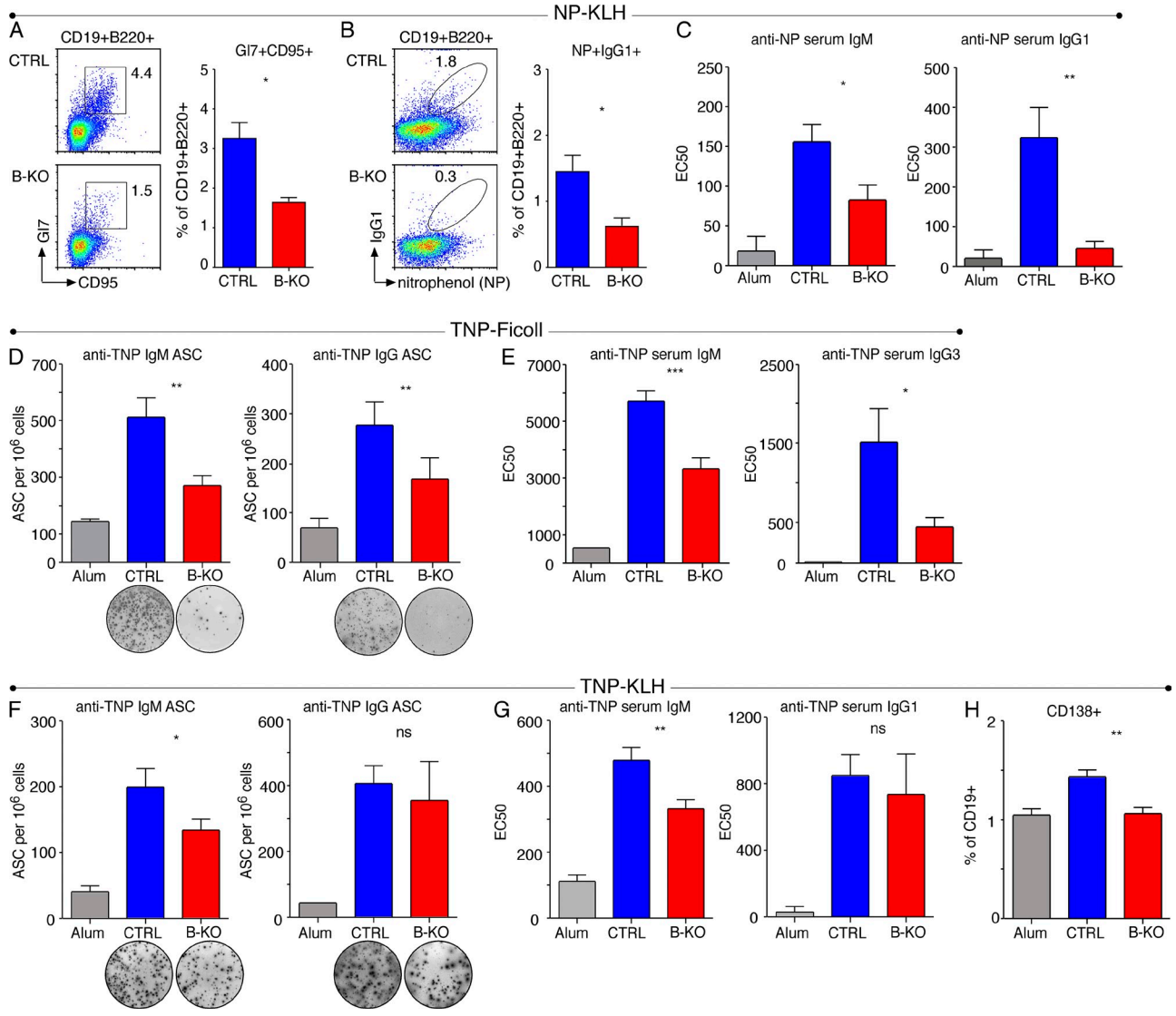

Figure 9. Absence of Kidins220 reduces the B cell response in vivo. (A) CTRL and B-KO mice were immunized with NP-KLH (λ- and T-dependent immunization) and analyzed after 6 d. The frequency of splenic GC B cells ($CD19^+B220^+GL7^+CD95^+$) is plotted as mean ± SEM from four to five mice per group. (B) Frequency of splenic NP-reactive IgG1-switched B cells of the mice as in A. (C) ELISA of NP-specific IgM (left) and IgG1 (right) in CTRL mice immunized only with aluminum hydroxide (Alum) or CTRL and B-KO mice immunized with NP-KLH from the mice shown in A. (D) CTRL and B-KO mice were immunized with TNP-Ficoll (λ-independent, T-independent immunization) and Alum. ELISPOT analysis of splenic TNP-specific IgM-secreting cells (left) and TNP-specific IgG-secreting cells (right) at 7 d after immunization. CTRL mice injected only with Alum served as a CTRL. Data of two independent experiments were pooled, and the mean ± SEM from six mice per group is shown. (E) ELISA of TNP-specific IgM (left) and IgG3 (right) from the mice shown in D. (F) CTRL and B-KO mice were immunized with TNP-KLH (λ-independent, T-dependent immunization) and Alum. ELISPOT analysis of splenic TNP-specific IgM-secreting cells (left) and TNP-specific IgG-secreting cells (right) 7 d after immunization. CTRL mice injected with Alum served as a CTRL. Data of two independent experiments were pooled, and the mean ± SEM from four to eight mice per group is plotted. (G) Serum titers of TNP-specific IgM (left) and IgG1 (right) from the mice shown in F measured by ELISA. (H) The percentage of $CD138^+$ B cells upon immunization as in F is shown. Two-tailed Student's *t* test (ns, $P > 0.05$; *, $P < 0.05$; **, $P < 0.01$; ***, $P < 0.001$).

immunization the anti-TNP IgG ASC and anti-TNP IgG1 serum titers were similar to the CTRLs (Fig. 9, F and G). The same held true for the GC reaction, measured as $GL7^+CD95^+$ cells by flow cytometry (not depicted). The percentage of plasma cells measured as $CD19^+CD138^+$ was decreased in the B-KO mice. Altogether, these results (a) support that the observed decrease in λ^+ B cells is indeed physiologically relevant and (b) clearly demonstrate that T-independent and early T-dependent responses are impaired in mice lacking Kidins220 expression in B cells.

DISCUSSION

In this study, we identified Kidins220 as a novel interaction partner of the resting and stimulated BCR and show that it

regulates BCR signaling. Although Kidins220 expression was first thought to be restricted to the nervous system (Iglesias et al., 2000), expression has now also been demonstrated for T (Jean-Mairet et al., 2011; Deswal et al., 2013) and B cells (this study).

In neurons, Kidins220 binds to TrkA, and this association is increased upon stimulation (Arévalo et al., 2004). Similarly, we have observed an enhanced Kidins220–BCR interaction upon BCR triggering. However, induction of phosphorylation by the pan-phosphatase inhibitor pervanadate (Campbell et al., 1995; Wienands et al., 1996) did not result in increased Kidins220–BCR association. In addition, antibody binding to the BCR in the presence of the Src-kinase inhibitor PP2 (Hanke et al., 1996), which impaired BCR phosphorylation and downstream signaling, still enhanced BCR–Kidins220 interaction. Because ligand binding to the BCR might induce structural changes within preformed BCR clusters (Schamel and Reth, 2000; Yang and Reth, 2010), we suggest that structural changes and/or Src-independent signaling promotes further association of Kidins220 with the BCR.

Analysis of BCR signaling in the absence of Kidins220 revealed that phosphorylation of Lyn, Syk, and PLCγ2 was reduced and Ca^{2+} mobilization diminished. Phosphorylation of SLP65 by Syk is required for efficient recruitment and activation of PLCγ2 and subsequent Ca^{2+} mobilization (Koretzky et al., 2006). Thus, it is plausible that in the absence of Kidins220 SLP65 is not properly phosphorylated and PLCγ2 suboptimally activated. Additionally, Kidins220 binds to and becomes phosphorylated by PKD in neurons (Iglesias et al., 2000). In B cells, PKD (formerly known as PKCμ) interacts with the BCR, Syk, and PLCγ2, and its activation relies on the presence of PLCγ2-produced DAG (Sidorenko et al., 1996). Therefore, the BCR–Kidins220 interaction might promote association with Syk, PLCγ2, and PKD, thereby supporting the activation of PLCγ2 and PKD.

Impaired activation of PLCγ2 reduces Ras–Erk pathway activation (Wheeler et al., 2013). Accordingly, in shKidins220 cells, B-Raf and Raf-1 were poorly activated upon BCR stimulation as estimated by their impaired phosphorylation-dependent gel retardation (Brummer et al., 2003; Dougherty et al., 2005). In addition, phosphorylation at S338, a critical residue for Raf-1 activation (Mason et al., 1999; Brummer et al., 2002; Dhillon et al., 2002) was hardly detected in the absence of Kidins220. These data suggest that functional coupling of the BCR to the Raf kinases requires Kidins220. Importantly, phosphorylation of Mek, the common substrate of Raf-1 and B-Raf, was strongly reduced and accompanied by reduced Erk phosphorylation in shKidins220 cells and primary B-KO cells.

Commensurate with impaired Erk activation, induction of its target gene products, c-Fos and CD69, was strongly reduced in the absence of Kidins220. B-KO cells showed reduced cell proliferation upon BCR stimulation, whereas proliferation toward the TLR9 ligand CpG was normal. Stimulation of the PI3K–Akt pathway upon BCR triggering was only partially diminished by the absence of Kidins220, being also in line with a similar B cell survival ex vivo. The BCAP–PI3K–Akt pathway is activated upon BCR triggering by direct Nck recruitment to the phosphorylated BCR (Castello et al., 2013). It is plausible that low levels of BCR phosphorylation permit activation of this pathway. In contrast, a low level of Syk activity might not suffice to optimally activate the PLCγ2–Ca^{2+} pathway. Our ex vivo results are further supported by the impaired activation of B cells in vivo. We found reduced T cell–independent and early T cell–dependent responses upon immunization with a non-λLC restricted antigen. Altogether, our data show that Kidins220 specifically couples the BCR to the Ca^{2+} and Ras–Erk pathways and therefore is crucial for optimal BCR-mediated cellular activation.

The embryonic lethality of the Kidins220 deficiency precluded analysis of B cell development. Thus, we used two alternative approaches: (1) fetal liver chimeras, as the Kidins220$^{-/-}$ embryos are unaltered until E14.5 (Cesca et al., 2012), including the percentages of hematopoietic and B cell–primed precursors, and (2) B cell–specific deletion of Kidins220 (named B-KO) achieved by breeding Kidins220^{fl} with mb1^{Cre} mice, promoting deletion in the pro–B cell stage (Hobeika et al., 2006). Mice reconstituted with Kidins220$^{-/-}$ fetal liver cells showed strongly reduced numbers of B cells in the BM. Furthermore, B cells lacking Kidins220 have a competitive disadvantage in BM repopulation. However, B cell numbers were only slightly reduced in the B-KO mice. This suggests that Kidins220 has an important role in development before B cell commitment that deserves further investigation.

Despite these quantitative differences, we found that Kidins220 is involved in regulating several steps in the development of B cells. During B cell development the pre-BCR and the BCR transmit signals using the Ras–Erk pathway (Fleming and Paige, 2001; Rowland et al., 2010a). Indeed, constitutive activation of this pathway mediates survival of pre–B cells in vivo (Nagaoka et al., 2000) and rescued reduced levels of antigen-independent BCR signaling (Rowland et al., 2010a). Our data support a model in which Kidins220 links the pre-BCR and BCR to the Ras–Erk pathway during development and immune responses. Our arguments will follow the stepwise analysis of B cell development.

First, the absolute number of pro–B cells was unaffected by the absence of Kidins220 in B-KO mice. Because survival and proliferation of pro–B cells depend on IL-7 (Cumano et al., 1990), Kidins220 might not play a role in IL-7R signaling.

Second, the number of pre–B cells was reduced. The pre-BCR activates the Ras–Erk pathway and allows cells to proliferate in response to IL-7, resulting in a population of cycling large pre–B cells (Fleming and Paige, 2001). At this stage, the κ locus is activated and, in the case of successful rearrangement, cells will exit this compartment expressing a κLC-containing IgM-BCR (Engel et al., 1999). B cell proliferation in the presence of IL-7 was normal in the absence of Kidins220, and those cells that exited the BM expressed a κLC-containing BCR. Thus, most likely, impaired proliferation of pre–B cells in the presence of IL-7 was not responsible for the reduced proportion of these cells in the B-KO mice. In the absence of a successfully assembled IgM-BCR, signals from the pre-BCR are

then crucial to activate the λ locus (Dingjan et al., 2001; Bai et al., 2007) and to promote survival ensuring a life span long enough for λLC rearrangement (Arakawa et al., 1996; Derudder et al., 2009). Importantly, pre–B cells from B-KO mice exhibited reduced survival upon withdrawal of IL-7 in vitro, and expression of the λLC was absent in B cells lacking Kidins220. Similarly, mice deficient in Btk or PLCγ2 have reduced numbers of λ^+ B cells (Dingjan et al., 2001; Bai et al., 2007), supporting genetically that Kidins220 is part of the Btk/PLCγ2 signaling module leading to activation of the λ locus. Altogether, these data support a model in which pre-BCR signaling is impaired in the absence of Kidins220, leading to a reduced life span of pre–B cells and precluding the rearrangement of and expression from the λ locus.

Third and alternatively, reduction of λ^+ cells could be caused by impaired BCR signals in immature B cells that control central tolerance in the BM. Upon IgM-BCR expression, BCR specificity will be tested for autoantigen recognition (Grandien et al., 1994). In the case of binding to an autoantigen, the BCR will transmit signals to initiate receptor editing to ensure that the cells expressing an autoreactive receptor do not leave the BM (Tiegs et al., 1993). New LC rearrangements might replace the autoreactive BCR for an innocuous one (Nemazee, 2006). Hence, efficient receptor editing leads to an increase in the use of λLC (Gay et al., 1993). BCR signaling in the absence of Kidins220 is reduced; thus, the threshold to initiate receptor editing might not be reached. An impairment in central tolerance would explain the observed reduction of λ^+ cells and would possibly result in autoantibody production. To test this hypothesis, we analyzed serum from Kidins220 KO and CTRL mice for antibodies reactive to dsDNA. We did not detect enhanced presence of autoantibodies in young B-KO mice (unpublished data). The short life span of the B-KO mice precludes analysis in older mice that might accumulate autoantibodies. Nevertheless, the reduction of λ^+ B cells is physiologically relevant because B-KO mice cannot mount an effective primary anti-NP immune response that is dominated by BCRs containing the λLC.

Fourth, the differentiation of immature B cells into transitional B cells and their export from the BM depends on BCR-induced Erk activation (Rowland et al., 2010b). In B-KO mice transitional B cell populations in the BM and the spleen were significantly reduced, suggesting that suboptimal BCR signaling might preclude efficient B cell export from the BM and population of the periphery.

Fifth, we found an increased proportion of MZ B cells and their precursors in the spleen. In several animal models reduced output of B cells from the BM is accompanied by a proportionally enlarged MZ population ("bottleneck" model; Martin and Kearney, 2002). This could be a compensatory mechanism to ensure the maintenance of the quick responding MZ "effector" B cells. In an alternative model the signal strength from the BCR at the transitional B cell stages defines whether the B cell develops into an FO cell (strong strength) or MZ B cell (weak strength; Pillai and Cariappa, 2009). A weaker BCR signaling strength might prone transitional B cells to develop into MZ B cells (reviewed in Pillai and Cariappa [2009]). Indeed, the MZ B cell compartment was also increased in the mixed fetal liver–reconstituted mice. However, in those mice WT cells compensate for the total output from the BM. Thus, we favor a scenario in which reduced BCR signaling results in a skewed development toward MZ B cells. This is in line with the SLP65 KO mice (Jumaa et al., 1999; Gerlach et al., 2003).

Sixth, it was suggested that the mature B cell pool (B2 or FO cells) requires tonic BCR signals for its maintenance (Lam et al., 1997; Kraus et al., 2004). We observed reduced numbers of mature B cells in the spleens, PC, and LNs of the B-KO mice, which might result from the reduced output from the BM and suboptimal B cell survival in the periphery. Although the last deserves deeper investigation, it might once more link Kidins220 to the transmission of BCR signals.

Lastly, T-independent and early T-dependent B cell immune responses were reduced in Kidins220 B-KO mice. However, late T-dependent responses (switch to IgG isotypes) were similar to the WT mice, suggesting that T cell help compensates for the defective BCR activation. Moreover, BCR internalization and antigen presentation on MHCII were normal in cells from the B-KO mice (unpublished data), indicating that Kidins220 does not globally regulate B cell functioning.

We did not find experimental evidence for Kidins220 playing a role in signaling downstream of other receptors expressed in the B cell linage, such as the BAFFR (unpublished data), IL-7R, or TLR9. Hence, our results provide strong evidence that Kidins220 specifically regulates pre-BCR and BCR signaling in B cells.

MATERIALS AND METHODS

Cells and mice. The mouse B cell line K46 and its NP-specific mIgD- and mIgM-BCR–expressing transfectants K46Lδm and K46Lμm, respectively, were previously described (Kim et al., 1979; Justement et al., 1990). The mouse plasmacytoma line J558L and the different NP-specific BCR isotype–expressing transfectants J558Lδm/mb1flN, J558Lμm/mb1flN, and J558Lγ2am/mb1 were also described previously (Oi et al., 1983; Hombach et al., 1988; Schamel and Reth, 2000). These cells were cultured in RPMI 1640 complete medium supplemented with 10% FCS, 2 mM L-glutamine, 100 U/ml penicillin/streptomycin, 10 mM Hepes, and 50 mM 2-mercaptoethanol and grown at 37°C in a humidified atmosphere with 5% CO_2. K46 transfectants were grown under 1 μg/ml MPA selection supplemented with 1.2 mM xanthine and 0.11 mM hypoxanthine. Cells expressing shKidins220 or shScrambled were selected and maintained with 2.5 μg/ml puromycin.

The B1-8/IEKT, C57BL/6Jax, C57BL/6Rag$^{-/-}$γc$^{-/-}$, C57BL/6-Ly5.1, and Kidins220mb1hCre mice were bred under specific pathogen–free conditions. The Kidins220$^{+/-}$ and Kidins220$^{+/fl}$ mice (Cesca et al., 2012) were provided by G. Schiavo (University College London, London, England, UK). The B1-8/IEKT mice (Takeda et al., 1993; Sonoda et al., 1997) and the mb1hCre mice (Hobeika et al., 2006) were described previously. All of them were backcrossed to C57BL/6 for at least 10 generations. Mice were sex and age matched with litter CTRLs whenever possible. All animal protocols (G12/64) were performed according to the German animal protection law with permission from the Veterinär und Lebensmittelüberwachungsbehörde Freiburg.

Mass spectrometry. The protein G–bead-purified IgG2a-BCR of K46 cells (and copurified proteins) were reduced by 1 mM DTT, alkylated using 5.5 mM iodoacetamide, and separated by SDS-PAGE. Gel lanes were cut into 10 equal slices, samples in-gel digested using trypsin (Promega), and resulting peptides processed on STAGE tips as described previously (Sprenger et al., 2013).

Peptides were analyzed by LC-MS/MS on a nanoscale-HPLC Agilent 1200 (Agilent Technologies) connected online to an LTQ-Orbitrap XL mass spectrometer (Thermo Fisher Scientific). All full-scan acquisition was performed in the FT-MS part of the mass spectrometer in the range from m/z 350 to 2,000 with an automatic gain CTRL target value of 106 and at resolution 60,000 at m/z 400. MS/MS acquisition was performed on the five most intense ions of the full scan in the LTQ using the following parameters: AGC target value, 5,000; ion selection thresholds, 1,000 counts; and maximum fill time, 100 ms. Wide-band activation was enabled with an activation q = 0.25 applied for 30 ms at a normalized collision energy of 35%. Singly charged ions and ions with unassigned charge states were excluded from MS/MS. Dynamic exclusion was applied. All recorded LC-MS/MS raw files were processed together in MaxQuant (Cox and Mann, 2008). Database searches were performed with the following parameters: mass accuracy thresholds were 0.5 D (MS/MS) and 6 ppm (precursor), maximum two missed cleavages were allowed, carbamidomethylation of cysteine as fixed modification, and deamidation (N/Q), oxidation (M), phosphorylation (STY), and protein N-terminal acetylation were set as variable modifications. MaxQuant was used to filter the identifications for a false discovery rate below 1% for peptides and proteins using forward-decoy searching.

Flow cytometry. Lymphocytes were isolated from the organs and erythrocytes removed by incubation in erythrocyte lysis buffer, 150 mM NH_4Cl and 10 mM $KHCO_3$, for 2–4 min at room temperature. 0.3×10^6 cells were stained on ice and in the dark for a minimum of 20 min in PBS containing 1% FCS and the indicated antibodies. Before analysis, cells were washed a minimum of two times. Measurements were performed using a Gallios (Beckham Coulter), Cyan (Beckham Coulter), or LSRII (BD) flow cytometer. Data were analyzed with FlowJo 6.1 software.

Antibodies. The following antibodies were used for WT: anti-Kidins220 (Proteintech), anti–Ig-α (Gold et al., 1991; provided by M. Gold, University of British Columbia, Vancouver, British Columbia, Canada), anti–Ig-β, anti–p-PLCγ2, anti–c-Fos, anti–p-Akt, and anti-Actin (all from Santa Cruz Biotechnology, Inc.); anti–λLC-HRPO and anti–κLC-HRPO (both from SouthernBiotech); anti-GAPDH (Sigma-Aldrich); and anti-pRaf, anti–p-Erk1/2, and anti–p-Mek antibodies (all from Cell Signaling Technology). Anti–Raf-1 (C12) and anti–B-Raf antibodies (H145 for IP, F7 for detection) were purchased from Santa Cruz Biotechnologies, Inc.

The following antibodies were used for flow cytometry: FITC-labeled anti-B220 and FITC-labeled anti-IgD (both from SouthernBiotech); PECy7-labeled anti-B220, PE-labeled anti-IgM, PE-labeled anti-cKit, APC-labeled anti-CD5, biotin-labeled anti-CD21, FITC-labeled anti-CD19, PE-labeled anti-CD23, and PE-labeled anti-CD43 (all from eBioscience); DL649-labeled anti–IgM Fab'_2 (all from Jackson ImmunoResearch Laboratories, Inc.); PECy7-labeled anti-IgM, FITC-labeled anti-λLC, APC-labeled anti-CD21, biotin-labeled anti-CD34, V450-labeled anti-CD45.2, FITC-labeled anti-CD45.1, FITC-labeled anti-Gl7, PE-labeled anti-CD95, and anti-IgG1 (all from BD); and PB-labeled anti-CD19, PECy7-labeled anti-CD23, and APC-labeled anti-CD93 (all from BioLegend). NP-BSA-biotin was obtained from Biosearch Technologies.

Cell stimulation and protein purifications. Cells were starved for 1 h and then stimulated for the indicated times at 37°C with 3 μg/ml anti-λLC–biotin (SouthernBiotech), 10 μg/ml anti-idiotypic Ac146 (Reth et al., 1978), or 3 μg/ml anti–mouse IgM Fab'_2 (Dianova) antibodies or with 25 μM pervanadate for 3 min. Treatment with the Src kinase inhibitor PP2 (Sigma-Aldrich) was performed at a concentration of 20 μM for 30 min at 37°C before stimulation. For BCR purifications, cells were lysed at a maximum of 40×10^6 cells/ml in 1 ml lysis buffer containing 0.5% Brij96V as described previously (Adachi et al., 1996), whereas RIPA buffer was used for lysate preparations. 40 μl was kept as a lysate CTRL. BCRs were purified from postnuclear supernatants by incubation with protein G–Sepharose or NP-coupled beads for 1–3 h at 4°C. MHCI was purified with the antibody SF1-1.1 (BD) and protein G–Sepharose. Raf immunoprecipitations were performed as described previously (Brummer et al., 2002). Phospho-tyrosine immunoprecipitations were performed with PT-66 Sepharose (Sigma-Aldrich). Band intensities were quantified using the ImageQuant TL software.

B cell purification and Ca^{2+} flux. Lymphocytes were isolated from the organs, and erythrocytes were removed by incubation in erythrocyte lysis buffer, 150 mM NH_4Cl/10 mM $KHCO_3$, for 2–4 min at room temperature. Untouched B cells were purified using the MACS B cell isolation kit (Miltenyi Biotech). Purity was >90%, as confirmed by flow cytometry using anti-CD19.

For Ca^{2+} flux analysis, cells were labeled in the dark with 5 μg/ml Indo-1 and 0.5 μg/ml Pluronic F-127 (both from Molecular Probes, Life Technologies) for 45 min in RPMI containing 1% FCS. Cells were washed and kept on ice in RPMI 1% FCS until measurement. The baseline was recorded, and cells were stimulated with the indicated antibody. The change of the ratio of Ca^{2+}-bound versus Ca^{2+}-unbound Indo-1 was followed for 5 min with an LSRII fluorescence spectrometer (BD). Data were analyzed with FlowJo 6.1 software.

Ex vivo experiments and IL-7 BM cultures. For ex vivo experiments, cells were kept in RPMI containing 10% FCS, 2 mM L-glutamine, 100 U/ml penicillin/streptomycin, 10 mM Hepes, and 50 mM 2-mercaptoethanol at 37°C in a humidified atmosphere with 5% CO_2. For ex vivo activations, purified B cells (0.10^6/sample) were incubated with different concentrations of anti–IgM Fab'_2 fragments (Dianova) for 11 h and then stained with PB-labeled anti-CD19 (BioLegend), PECy7-labeled anti-CD69 (eBioscience) or PE-labeled anti-CD69 (eBioscience), and PE-labeled anti-CD86 (BioLegend).

For proliferation experiments, purified B cells (0.2×10^6/sample) were labeled with CFSE in PBS containing 0.5% BSA according to the manufacturer's instructions (Invitrogen) for 10 min at 37°C in the dark and 5 min on ice. After 3 d in culture with the appropriate stimulus (1 μg/ml anti–IgM Fab'_2 fragments or 2.5 μg/ml CpG [ODN 1668; InvivoGen]) in the presence of 0.5 ng/ml IL-4 (PeproTech), cells were stained with PB-labeled anti-CD19 (BioLegend). CFSE fluorescence of the $CD19^+$ cells was measured by flow cytometry.

BM cultures were prepared from freshly isolated BM cells after erythrocyte lysis. Cells were cultured in IMDM containing 10% FCS, 100 U/ml penicillin/streptomycin, 50 mM 2-mercaptoethanol, and IL-7 at 37°C with 7.5% CO_2 for 1 wk. Then the culture was split and grown either with or without IL-7. Survival and surface receptor expression were analyzed by flow cytometry.

Fetal liver reconstitution. For the fetal liver reconstitution experiments, female $Kidins220^{+/-}$ mice were mated with male $Kidins220^{+/-}$ mice. Embryos were taken and fetal liver cells isolated on E12.5, E13.5, or E14.5. Equal numbers of Kidins220 KO and WT fetal liver cells were matched for the embryonic developmental stage and injected into sublethally (400 rad) irradiated $Rag^{-/-}\gamma\chi^{-/-}$ mice. After 2 mo, the animals were killed and analyzed for reconstitution. For competitive reconstitution experiments, embryos obtained from WT CD45.1 mice were used.

Immunization, ELISA, and ELISPOT assay. To immunize mice, 4-hydroxy-3-NP coupled to KLH (NP_{28}-KLH), 2,4,6-TNP conjugated to KLH (TNP_{20}-KLH), and TNP conjugated to AECM-Ficoll (TNP_{36}-Ficoll; all from Biosearch Technologies) were alum precipitated by mixing them (1 mg/ml) with an aluminum hydroxide solution at a 1:1 ratio. Mice were immunized i.p. with 376 μg per 100 g body weight. After 6–7 d, serum was collected and the mice were killed, and single-cell suspensions of the spleen were used for the ELISPOT assay and analyzed by flow cytometry. Titers of antigen-specific antibodies were measured by ELISA. In brief, plates were coated with antigen (NP_{15}-BSA or TNP_{13}-BSA from Biosearch Technologies) for the capture of the serum antibodies, and goat anti–mouse HRPO-conjugated antibodies were used for detection (IgM, IgG, IgG1, and IgG3; all from SouthernBiotech). Each serum sample was serially diluted and absorbance at 405 nm measured. Data were adjusted to best-fit sigmoidal curve and the EC_{50} calculated using GraphPad Prism software. For ELISPOT, spleen single-cell suspensions were incubated for 16 h in multiscreen filtration plates (EMD Millipore) previously coated with antigen (NP_{15}-BSA or

TNP_{13}-BSA). ASCs were detected by incubation with goat anti–mouse HRPO-conjugated antibodies (IgM or IgG; from SouthernBiotech) and subsequently with 3-amino-9-ethyl-carbazole (Sigma-Aldrich). Spots were counted using an automated reader.

We appreciate the BIOSS toolbox for providing us with reagents. We thank C. Johner, U. Stauffer, N. Joswig, N. Knoll, J. Hülsdünker, K. Fehrenbach, E. Dengler, E. Levit, C. Schell, T. Huber, and S. Braun for experimental help; M. Gold for providing the anti-Igα antiserum; G. Schiavo for the Kidins220-deficient mice; F. Batista, A. Izcue, and S. Infantino for sharing procedures; and J. Wienands, L. Nitschke, P. Nielsen, S. Deswal, and R. Pelanda for discussions.

This work was supported by the German Research Foundation (DFG) through the Excellence Initiative GSC-4 (Spemann Graduate School of Biology and Medicine) and EXC294 (BIOSS) to G.J. Fiala, J. Dengjel, T. Brummer, M. Reth, and W.W.A. Schamel. T. Brummer was supported by the Emmy-Noether Program of the DFG. S. Minguet was supported by the DFG through SFB1160 and M. Reth by ERC grant 32297 and by the DFG through SFB746 and TRR130.

The authors declare no competing financial interests.

Submitted: 3 July 2014
Accepted: 14 August 2015

REFERENCES

Adachi, T., W.W. Schamel, K.M. Kim, T. Watanabe, B. Becker, P.J. Nielsen, and M. Reth. 1996. The specificity of association of the IgD molecule with the accessory proteins BAP31/BAP29 lies in the IgD transmembrane sequence. *EMBO J.* 15:1534–1541.

Allman, D., R.C. Lindsley, W. DeMuth, K. Rudd, S.A. Shinton, and R.R. Hardy. 2001. Resolution of three nonproliferative immature splenic B cell subsets reveals multiple selection points during peripheral B cell maturation. *J. Immunol.* 167:6834–6840. http://dx.doi.org/10.4049/jimmunol.167.12.6834

Arakawa, H., T. Shimizu, and S. Takeda. 1996. Re-evaluation of the probabilities for productive arrangements on the κ and λ loci. *Int. Immunol.* 8:91–99. http://dx.doi.org/10.1093/intimm/8.1.91

Arévalo, J.C., H. Yano, K.K. Teng, and M.V. Chao. 2004. A unique pathway for sustained neurotrophin signaling through an ankyrin-rich membrane-spanning protein. *EMBO J.* 23:2358–2368. http://dx.doi.org/10.1038/sj.emboj.7600253

Bai, L., Y. Chen, Y. He, X. Dai, X. Lin, R. Wen, and D. Wang. 2007. Phospholipase Cγ2 contributes to light-chain gene activation and receptor editing. *Mol. Cell. Biol.* 27:5957–5967. http://dx.doi.org/10.1128/MCB.02273-06

Brummer, T., P.E. Shaw, M. Reth, and Y. Misawa. 2002. Inducible gene deletion reveals different roles for B-Raf and Raf-1 in B-cell antigen receptor signalling. *EMBO J.* 21:5611–5622. http://dx.doi.org/10.1093/emboj/cdf588

Brummer, T., H. Naegele, M. Reth, and Y. Misawa. 2003. Identification of novel ERK-mediated feedback phosphorylation sites at the C-terminus of B-Raf. *Oncogene.* 22:8823–8834. http://dx.doi.org/10.1038/sj.onc.1207185

Campbell, K.S., W.D. Bedzyk, and J.C. Cambier. 1995. Manipulation of B cell antigen receptor tyrosine phosphorylation using aluminum fluoride and sodium orthovanadate. *Mol. Immunol.* 32:1283–1294. http://dx.doi.org/10.1016/0161-5890(95)00088-7

Castellanos, M.C., C. Muñoz, M.C. Montoya, E. Lara-Pezzi, M. López-Cabrera, and M.O. de Landázuri. 1997. Expression of the leukocyte early activation antigen CD69 is regulated by the transcription factor AP-1. *J. Immunol.* 159:5463–5473.

Castello, A., M. Gaya, J. Tucholski, T. Oellerich, K.H. Lu, A. Tafuri, T. Pawson, J. Wienands, M. Engelke, and F.D. Batista. 2013. Nck-mediated recruitment of BCAP to the BCR regulates the PI(3)K-Akt pathway in B cells. *Nat. Immunol.* 14:966–975. http://dx.doi.org/10.1038/ni.2685

Cesca, F., A. Yabe, B. Spencer-Dene, A. Arrigoni, M. Al-Qatari, D. Henderson, H. Phillips, M. Koltzenburg, F. Benfenati, and G. Schiavo. 2011. Kidins220/ARMS is an essential modulator of cardiovascular and nervous system development. *Cell Death Dis.* 2:e226. http://dx.doi.org/10.1038/cddis.2011.108

Cesca, F., A. Yabe, B. Spencer-Dene, J. Scholz-Starke, L. Medrihan, C.H. Maden, H. Gerhardt, I.R. Orriss, P. Baldelli, M. Al-Qatari, et al. 2012. Kidins220/ARMS mediates the integration of the neurotrophin and VEGF pathways in the vascular and nervous systems. *Cell Death Differ.* 19:194–208. http://dx.doi.org/10.1038/cdd.2011.141

Chang, M.S., J.C. Arevalo, and M.V. Chao. 2004. Ternary complex with Trk, p75, and an ankyrin-rich membrane spanning protein. *J. Neurosci. Res.* 78:186–192. http://dx.doi.org/10.1002/jnr.20262

Cox, J., and M. Mann. 2008. MaxQuant enables high peptide identification rates, individualized p.p.b.-range mass accuracies and proteome-wide protein quantification. *Nat. Biotechnol.* 26:1367–1372. http://dx.doi.org/10.1038/nbt.1511

Cumano, A., K. Dorshkind, S. Gillis, and C.J. Paige. 1990. The influence of S17 stromal cells and interleukin 7 on B cell development. *Eur. J. Immunol.* 20:2183–2189. http://dx.doi.org/10.1002/eji.1830201006

Derudder, E., E.J. Cadera, J.C. Vahl, J. Wang, C.J. Fox, S. Zha, G. van Loo, M. Pasparakis, M.S. Schlissel, M. Schmidt-Supprian, and K. Rajewsky. 2009. Development of immunoglobulin λ-chain–positive B cells, but not editing of immunoglobulin κ-chain, depends on NF-κB signals. *Nat. Immunol.* 10:647–654. http://dx.doi.org/10.1038/ni.1732

Deswal, S., A. Meyer, G.J. Fiala, A.E. Eisenhardt, L.C. Schmitt, M. Salek, T. Brummer, O. Acuto, and W.W. Schamel. 2013. Kidins220/ARMS associates with B-Raf and the TCR, promoting sustained Erk signaling in T cells. *J. Immunol.* 190:1927–1935. http://dx.doi.org/10.4049/jimmunol.1200653

Dhillon, A.S., S. Meikle, Z. Yazici, M. Eulitz, and W. Kolch. 2002. Regulation of Raf-1 activation and signalling by dephosphorylation. *EMBO J.* 21:64–71. http://dx.doi.org/10.1093/emboj/21.1.64

Dingjan, G.M., S. Middendorp, K. Dahlenborg, A. Maas, F. Grosveld, and R.W. Hendriks. 2001. Bruton's tyrosine kinase regulates the activation of gene rearrangements at the lambda light chain locus in precursor B cells in the mouse. *J. Exp. Med.* 193:1169–1178. http://dx.doi.org/10.1084/jem.193.10.1169

Dougherty, M.K., J. Müller, D.A. Ritt, M. Zhou, X.Z. Zhou, T.D. Copeland, T.P. Conrads, T.D. Veenstra, K.P. Lu, and D.K. Morrison. 2005. Regulation of Raf-1 by direct feedback phosphorylation. *Mol. Cell.* 17:215–224. http://dx.doi.org/10.1016/j.molcel.2004.11.055

Engel, H., A. Rolink, and S. Weiss. 1999. B cells are programmed to activate κ and λ for rearrangement at consecutive developmental stages. *Eur. J. Immunol.* 29:2167–2176. http://dx.doi.org/10.1002/(SICI)1521-4141(199907)29:07<2167::AID-IMMU2167>3.0.CO;2-H

Fleming, H.E., and C.J. Paige. 2001. Pre-B cell receptor signaling mediates selective response to IL-7 at the pro-B to pre-B cell transition via an ERK/MAP kinase-dependent pathway. *Immunity.* 15:521–531. http://dx.doi.org/10.1016/S1074-7613(01)00216-3

Gay, D., T. Saunders, S. Camper, and M. Weigert. 1993. Receptor editing: an approach by autoreactive B cells to escape tolerance. *J. Exp. Med.* 177:999–1008. http://dx.doi.org/10.1084/jem.177.4.999

Gerlach, J., S. Ghosh, H. Jumaa, M. Reth, J. Wienands, A.C. Chan, and L. Nitschke. 2003. B cell defects in SLP65/BLNK-deficient mice can be partially corrected by the absence of CD22, an inhibitory coreceptor for BCR signaling. *Eur. J. Immunol.* 33:3418–3426. http://dx.doi.org/10.1002/eji.200324290

Gold, M.R. 2000. Intermediary signaling effectors coupling the B-cell receptor to the nucleus. *Curr. Top. Microbiol. Immunol.* 245:77–134.

Gold, M.R., L. Matsuuchi, R.B. Kelly, and A.L. DeFranco. 1991. Tyrosine phosphorylation of components of the B-cell antigen receptors following receptor crosslinking. *Proc. Natl. Acad. Sci. USA.* 88:3436–3440. http://dx.doi.org/10.1073/pnas.88.8.3436

Grandien, A., R. Fucs, A. Nobrega, J. Andersson, and A. Coutinho. 1994. Negative selection of multireactive B cell clones in normal adult mice. *Eur. J. Immunol.* 24:1345–1352. http://dx.doi.org/10.1002/eji.1830240616

Gross, J.A., J. Johnston, S. Mudri, R. Enselman, S.R. Dillon, K. Madden, W. Xu, J. Parrish-Novak, D. Foster, C. Lofton-Day, et al. 2000. TACI and BCMA are receptors for a TNF homologue implicated in B-cell autoimmune disease. *Nature.* 404:995–999. http://dx.doi.org/10.1038/35010115

Hanke, J.H., J.P. Gardner, R.L. Dow, P.S. Changelian, W.H. Brissette, E.J. Weringer, B.A. Pollok, and P.A. Connelly. 1996. Discovery of a novel, potent, and Src family-selective tyrosine kinase inhibitor. Study of Lck- and FynT-dependent T cell activation. *J. Biol. Chem.* 271:695–701. http://dx.doi.org/10.1074/jbc.271.2.695

Hashimoto, A., H. Okada, A. Jiang, M. Kurosaki, S. Greenberg, E.A. Clark, and T. Kurosaki. 1998. Involvement of guanosine triphosphatases and phospholipase C-γ2 in extracellular signal-regulated kinase, c-Jun NH_2-terminal kinase, and p38 mitogen-activated protein kinase activation by the B cell antigen receptor. *J. Exp. Med.* 188:1287–1295. http://dx.doi.org/10.1084/jem.188.7.1287

Hobeika, E., S. Thiemann, B. Storch, H. Jumaa, P.J. Nielsen, R. Pelanda, and M. Reth. 2006. Testing gene function early in the B cell lineage in mb1-cre mice. *Proc. Natl. Acad. Sci. USA.* 103:13789–13794. http://dx.doi.org/10.1073/pnas.0605944103

Hombach, J., L. Leclercq, A. Radbruch, K. Rajewsky, and M. Reth. 1988. A novel 34-kd protein co-isolated with the IgM molecule in surface IgM-expressing cells. *EMBO J.* 7:3451–3456.

Hombach, J., T. Tsubata, L. Leclercq, H. Stappert, and M. Reth. 1990. Molecular components of the B-cell antigen receptor complex of the IgM class. *Nature.* 343:760–762. http://dx.doi.org/10.1038/343760a0

Iglesias, T., N. Cabrera-Poch, M.P. Mitchell, T.J. Naven, E. Rozengurt, and G. Schiavo. 2000. Identification and cloning of Kidins220, a novel neuronal substrate of protein kinase D. *J. Biol. Chem.* 275:40048–40056. http://dx.doi.org/10.1074/jbc.M005261200

Jean-Mairet, R.M., C. López-Menéndez, L. Sánchez-Ruiloba, S. Sacristán, M. Rodríguez-Martínez, L. Riol-Blanco, P. Sánchez-Mateos, F. Sánchez-Madrid, J.L. Rodríguez-Fernández, M.R. Campanero, and T. Iglesias. 2011. The neuronal protein Kidins220/ARMS associates with ICAM-3 and other uropod components and regulates T-cell motility. *Eur. J. Immunol.* 41:1035–1046. http://dx.doi.org/10.1002/eji.201040513

Jumaa, H., B. Wollscheid, M. Mitterer, J. Wienands, M. Reth, and P.J. Nielsen. 1999. Abnormal development and function of B lymphocytes in mice deficient for the signaling adaptor protein SLP-65. *Immunity.* 11:547–554. http://dx.doi.org/10.1016/S1074-7613(00)80130-2

Justement, L.B., J. Wienands, J. Hombach, M. Reth, and J.C. Cambier. 1990. Membrane IgM and IgD molecules fail to transduce Ca^{2+} mobilizing signals when expressed on differentiated B lineage cells. *J. Immunol.* 144:3272–3280.

Kim, K.J., C. Kanellopoulos-Langevin, R.M. Merwin, D.H. Sachs, and R. Asofsky. 1979. Establishment and characterization of BALB/c lymphoma lines with B cell properties. *J. Immunol.* 122:549–554.

Kong, H., J. Boulter, J.L. Weber, C. Lai, and M.V. Chao. 2001. An evolutionarily conserved transmembrane protein that is a novel downstream target of neurotrophin and ephrin receptors. *J. Neurosci.* 21:176–185.

Koretzky, G.A., F. Abtahian, and M.A. Silverman. 2006. SLP76 and SLP65: complex regulation of signalling in lymphocytes and beyond. *Nat. Rev. Immunol.* 6:67–78. http://dx.doi.org/10.1038/nri1750

Kraus, M., M.B. Alimzhanov, N. Rajewsky, and K. Rajewsky. 2004. Survival of resting mature B lymphocytes depends on BCR signaling via the Igα/α heterodimer. *Cell.* 117:787–800. http://dx.doi.org/10.1016/j.cell.2004.05.014

Kurosaki, T. 1999. Genetic analysis of B cell antigen receptor signaling. *Annu. Rev. Immunol.* 17:555–592. http://dx.doi.org/10.1146/annurev.immunol.17.1.555

Lam, K.P., R. Kühn, and K. Rajewsky. 1997. In vivo ablation of surface immunoglobulin on mature B cells by inducible gene targeting results in rapid cell death. *Cell.* 90:1073–1083. http://dx.doi.org/10.1016/S0092-8674(00)80373-6

Loder, F., B. Mutschler, R.J. Ray, C.J. Paige, P. Sideras, R. Torres, M.C. Lamers, and R. Carsetti. 1999. B cell development in the spleen takes place in discrete steps and is determined by the quality of B cell receptor-derived signals. *J. Exp. Med.* 190:75–89. http://dx.doi.org/10.1084/jem.190.1.75

López-Menéndez, C., S. Gascón, M. Sobrado, O.G. Vidaurre, A.M. Higuero, A. Rodríguez-Peña, T. Iglesias, and M. Díaz-Guerra. 2009. Kidins220/ARMS downregulation by excitotoxic activation of NMDARs reveals its involvement in neuronal survival and death pathways. *J. Cell Sci.* 122:3554–3565. http://dx.doi.org/10.1242/jcs.056473

Mackay, F., S.A. Woodcock, P. Lawton, C. Ambrose, M. Baetscher, P. Schneider, J. Tschopp, and J.L. Browning. 1999. Mice transgenic for BAFF develop lymphocytic disorders along with autoimmune manifestations. *J. Exp. Med.* 190:1697–1710. http://dx.doi.org/10.1084/jem.190.11.1697

Mandal, M., S.E. Powers, K. Ochiai, K. Georgopoulos, B.L. Kee, H. Singh, and M.R. Clark. 2009. Ras orchestrates exit from the cell cycle and light-chain recombination during early B cell development. *Nat. Immunol.* 10:1110–1117. http://dx.doi.org/10.1038/ni.1785

Martin, F., and J.F. Kearney. 2002. Marginal-zone B cells. *Nat. Rev. Immunol.* 2:323–335. http://dx.doi.org/10.1038/nri799

Mason, C.S., C.J. Springer, R.G. Cooper, G. Superti-Furga, C.J. Marshall, and R. Marais. 1999. Serine and tyrosine phosphorylations cooperate in Raf-1, but not B-Raf activation. *EMBO J.* 18:2137–2148. http://dx.doi.org/10.1093/emboj/18.8.2137

McGuire, K.L., and E.S. Vitetta. 1981. κ/λ Shifts do not occur during maturation of murine B cells. *J. Immunol.* 127:1670–1673.

Minguet, S., M. Huber, L. Rosenkranz, W.W. Schamel, M. Reth, and T. Brummer. 2005. Adenosine and cAMP are potent inhibitors of the NF-κB pathway downstream of immunoreceptors. *Eur. J. Immunol.* 35:31–41. http://dx.doi.org/10.1002/eji.200425524

Minguet, S., E.P. Dopfer, C. Pollmer, M.A. Freudenberg, C. Galanos, M. Reth, M. Huber, and W.W. Schamel. 2008. Enhanced B-cell activation mediated by TLR4 and BCR crosstalk. *Eur. J. Immunol.* 38:2475–2487. http://dx.doi.org/10.1002/eji.200738094

Nagaoka, H., Y. Takahashi, R. Hayashi, T. Nakamura, K. Ishii, J. Matsuda, A. Ogura, Y. Shirakata, H. Karasuyama, T. Sudo, et al. 2000. Ras mediates effector pathways responsible for pre-B cell survival, which is essential for the developmental progression to the late pre-B cell stage. *J. Exp. Med.* 192:171–182. http://dx.doi.org/10.1084/jem.192.2.171

Nemazee, D. 2006. Receptor editing in lymphocyte development and central tolerance. *Nat. Rev. Immunol.* 6:728–740. http://dx.doi.org/10.1038/nri1939

Neubrand, V.E., F. Cesca, F. Benfenati, and G. Schiavo. 2012. Kidins220/ARMS as a functional mediator of multiple receptor signalling pathways. *J. Cell Sci.* 125:1845–1854. http://dx.doi.org/10.1242/jcs.102764

Oh-hora, M., S. Johmura, A. Hashimoto, M. Hikida, and T. Kurosaki. 2003. Requirement for Ras guanine nucleotide releasing protein 3 in coupling phospholipase C-γ2 to Ras in B cell receptor signaling. *J. Exp. Med.* 198:1841–1851. http://dx.doi.org/10.1084/jem.20031547

Oi, V.T., S.L. Morrison, L.A. Herzenberg, and P. Berg. 1983. Immunoglobulin gene expression in transformed lymphoid cells. *Proc. Natl. Acad. Sci. USA.* 80:825–829. http://dx.doi.org/10.1073/pnas.80.3.825

Pillai, S., and A. Cariappa. 2009. The follicular versus marginal zone B lymphocyte cell fate decision. *Nat. Rev. Immunol.* 9:767–777. http://dx.doi.org/10.1038/nri2656

Ray, R.J., A. Stoddart, J.L. Pennycook, H.O. Huner, C. Furlonger, G.E. Wu, and C.J. Paige. 1998. Stromal cell-independent maturation of IL-7-responsive pro-B cells. *J. Immunol.* 160:5886–5897.

Reth, M., G.J. Hämmerling, and K. Rajewsky. 1978. Analysis of the repertoire of anti-NP antibodies in C57BL/6 mice by cell fusion. I. Characterization of antibody families in the primary and hyperimmune response. *Eur. J. Immunol.* 8:393–400. http://dx.doi.org/10.1002/eji.1830080605

Richards, J.D., S.H. Davé, C.H. Chou, A.A. Mamchak, and A.L. DeFranco. 2001. Inhibition of the MEK/ERK signaling pathway blocks a subset of B cell responses to antigen. *J. Immunol.* 166:3855–3864. http://dx.doi.org/10.4049/jimmunol.166.6.3855

Rodriguez-Viciana, P., J. Oses-Prieto, A. Burlingame, M. Fried, and F. McCormick. 2006. A phosphatase holoenzyme comprised of Shoc2/Sur8 and the catalytic subunit of PP1 functions as an M-Ras effector to modulate Raf activity. *Mol. Cell.* 22:217–230. http://dx.doi.org/10.1016/j.molcel.2006.03.027

Rolink, A., and F. Melchers. 1991. Molecular and cellular origins of B lymphocyte diversity. *Cell.* 66:1081–1094. http://dx.doi.org/10.1016/0092-8674(91)90032-T

Rolink, A., A. Kudo, H. Karasuyama, Y. Kikuchi, and F. Melchers. 1991. Long-term proliferating early pre B cell lines and clones with the potential to develop to surface Ig-positive, mitogen reactive B cells in vitro and in vivo. *EMBO J.* 10:327–336.

Rolli, V., M. Gallwitz, T. Wossning, A. Flemming, W.W. Schamel, C. Zürn, and M. Reth. 2002. Amplification of B cell antigen receptor signaling by a Syk/ITAM positive feedback loop. *Mol. Cell.* 10:1057–1069. http://dx.doi.org/10.1016/S1097-2765(02)00739-6

Rowland, S.L., C.L. DePersis, R.M. Torres, and R. Pelanda. 2010a. Ras activation of Erk restores impaired tonic BCR signaling and rescues immature B cell differentiation. *J. Exp. Med.* 207:607–621. http://dx.doi.org/10.1084/jem.20091673

Rowland, S.L., K.F. Leahy, R. Halverson, R.M. Torres, and R. Pelanda. 2010b. BAFF receptor signaling aids the differentiation of immature B cells into transitional B cells following tonic BCR signaling. *J. Immunol.* 185:4570–4581. http://dx.doi.org/10.4049/jimmunol.1001708

Schamel, W.W., and M. Reth. 2000. Monomeric and oligomeric complexes of the B cell antigen receptor. *Immunity*. 13:5–14. http://dx.doi.org/10.1016/S1074-7613(00)00003-0

Shaw, A.C., W. Swat, R. Ferrini, L. Davidson, and F.W. Alt. 1999. Activated Ras signals developmental progression of recombinase-activating gene (RAG)-deficient pro-B lymphocytes. *J. Exp. Med.* 189:123–129.

Sidorenko, S.P., C.L. Law, S.J. Klaus, K.A. Chandran, M. Takata, T. Kurosaki, and E.A. Clark. 1996. Protein kinase C μ (PKCμ) associates with the B cell antigen receptor complex and regulates lymphocyte signaling. *Immunity*. 5:353–363. http://dx.doi.org/10.1016/S1074-7613(00)80261-7

Sonoda, E., Y. Pewzner-Jung, S. Schwers, S. Taki, S. Jung, D. Eilat, and K. Rajewsky. 1997. B cell development under the condition of allelic inclusion. *Immunity*. 6:225–233. http://dx.doi.org/10.1016/S1074-7613(00)80325-8

Sprenger, A., S. Weber, M. Zarai, R. Engelke, J.M. Nascimento, C. Gretzmeier, M. Hilpert, M. Boerries, C. Has, H. Busch, et al. 2013. Consistency of the proteome in primary human keratinocytes with respect to gender, age, and skin localization. *Mol. Cell. Proteomics*. 12:2509–2521. http://dx.doi.org/10.1074/mcp.M112.025478

Srivastava, B., W.J. Quinn III, K. Hazard, J. Erikson, and D. Allman. 2005. Characterization of marginal zone B cell precursors. *J. Exp. Med.* 202:1225–1234. http://dx.doi.org/10.1084/jem.20051038

Sugawara, H., M. Kurosaki, M. Takata, and T. Kurosaki. 1997. Genetic evidence for involvement of type 1, type 2 and type 3 inositol 1,4,5-trisphosphate receptors in signal transduction through the B-cell antigen receptor. *EMBO J.* 16:3078–3088. http://dx.doi.org/10.1093/emboj/16.11.3078

Takeda, S., Y.R. Zou, H. Bluethmann, D. Kitamura, U. Muller, and K. Rajewsky. 1993. Deletion of the immunoglobulin kappa chain intron enhancer abolishes kappa chain gene rearrangement in cis but not lambda chain gene rearrangement in trans. *EMBO J.* 12:2329–2336.

ten Boekel, E., F. Melchers, and A. Rolink. 1995. The status of Ig loci rearrangements in single cells from different stages of B cell development. *Int. Immunol.* 7:1013–1019. http://dx.doi.org/10.1093/intimm/7.6.1013

Tiegs, S.L., D.M. Russell, and D. Nemazee. 1993. Receptor editing in self-reactive bone marrow B cells. *J. Exp. Med.* 177:1009–1020. http://dx.doi.org/10.1084/jem.177.4.1009

Vettermann, C., K. Herrmann, C. Albert, E. Roth, M.R. Bösl, and H.M. Jäck. 2008. A unique role for the λ5 nonimmunoglobulin tail in early B lymphocyte development. *J. Immunol.* 181:3232–3242. http://dx.doi.org/10.4049/jimmunol.181.5.3232

Wheeler, M.L., M.B. Dong, R. Brink, X.P. Zhong, and A.L. DeFranco. 2013. Diacylglycerol kinase ζ limits B cell antigen receptor–dependent activation of ERK signaling to inhibit early antibody responses. *Sci. Signal.* 6:ra91. http://dx.doi.org/10.1126/scisignal.2004189

Wienands, J., O. Larbolette, and M. Reth. 1996. Evidence for a preformed transducer complex organized by the B cell antigen receptor. *Proc. Natl. Acad. Sci. USA*. 93:7865–7870. http://dx.doi.org/10.1073/pnas.93.15.7865

Wienands, J., J. Schweikert, B. Wollscheid, H. Jumaa, P.J. Nielsen, and M. Reth. 1998. SLP-65: a new signaling component in B lymphocytes which requires expression of the antigen receptor for phosphorylation. *J. Exp. Med.* 188:791–795.

Yang, J., and M. Reth. 2010. Oligomeric organization of the B-cell antigen receptor on resting cells. *Nature*. 467:465–469. http://dx.doi.org/10.1038/nature09357

Yasuda, T., H. Sanjo, G. Pagès, Y. Kawano, H. Karasuyama, J. Pouysségur, M. Ogata, and T. Kurosaki. 2008. Erk kinases link pre-B cell receptor signaling to transcriptional events required for early B cell expansion. *Immunity*. 28:499–508. http://dx.doi.org/10.1016/j.immuni.2008.02.015